九州大学学術情報リポジトリ
Kyushu University Institutional Repository

Disruption Process of Accumulated Northward Interplanetary Magnetic Fields Ahead of the Dayside Magnetosphere

橋本, 翼

https://hdl.handle.net/2324/7182304

出版情報：Kyushu University, 2023, 博士（理学）, 課程博士
バージョン：
権利関係：

KYUSHU UNIVERSITY

Department of Earth and Planetary Sciences
Graduate School of Science
KYUSHU UNIVERSITY

Disruption Process of Accumulated Northward Interplanetary Magnetic Fields Ahead of the Dayside Magnetosphere

Tsubasa Hashimoto

Abstract

The Interplanetary Magnetic Field (IMF) constantly continuing to blow toward the Earth interacts with the Earth's magnetic field. One of the interactions is the magnetic reconnection, allowing solar energy to flow into the Earth when the IMF connects to the Earth's magnetic field. The amount of energy injection into the Earth changes depending on the IMF direction, affecting the location and efficiency of the magnetic reconnection. It is important to understand the presence or absence of the reconnection associated with the IMF condition because a change in the plasma distribution in the ionosphere and the magnetosphere is triggered by the magnetic reconnection.

We focused on situations where the IMF direction changed discontinuously from northward to southward. Previous models and observations suggested that the IMF direction discontinuity (DD) led to the magnetic reconnection between northward and southward IMF when the DD reached the bow shock. However, there was little research on this reconnection because reconnected magnetic field lines did not directly connect with the Earth's magnetic field line. Then, the plasma and magnetic field structure changes associated with the IMF reconnection, as well as a quantitative assessment of its effects, is poorly understood. The purpose of this thesis is to simulate and visualize the effects on plasma and magnetic field structures and provide a quantitative interpretation through a comparison with the observation results by satellite data when IMF DD moves from the dayside to the nightside of the magnetosheath. We implemented the Reproduce Plasma Universe (REPPU) 3D Magnetohydrodynamic (MHD) code.

First, we elucidated the change in the magnetic field structures associated with the magnetic reconnection that occurred during the movement of the DD between the dayside and nightside magnetosphere. As shown by the previous work, we

indicated the occurrence of the reconnection when the IMF DD reached the bow shock. We called the magnetic field lines created by this reconnection the "U-shaped magnetic field line". The U-shaped magnetic field lines with both ends extending to the solar wind region were transported to the high-latitude magnetopause, where they reconnected with the lobe magnetic field.

We also conducted a quantitative study of the IMF reconnection outflow. Reconnected magnetic field lines are greatly bent and have curvature, it is known that the Ampère force generates the plasma acceleration as reconnection outflow. In the GEOTAIL observations, the plasma velocity accelerated toward the exhaust direction from the IMF reconnection region, by approximately 75 km/s, in response to the arrival of the IMF DD. We also obtained a similar variation from our simulation results. The representation of reconnection outflow increased by 20 km/s relative to the background magnetosheath flow velocity in the exhaust direction. However, this acceleration appeared to be slow as compared with the accelerated reconnection outflow in the nightside plasma sheet or the dayside magnetopause. A slow reconnection outflow velocity was due to the weak incoming IMF strength. Furthermore, the magnetic field lines after the IMF reconnection did not immediately move downstream from the reconnection region. Consequently, the IMF reconnection occurred intermittently, confirmed by the plasma flow perpendicular to the magnetic field after IMF reconnection.

We revealed the current circuit generated by the effects on the DD. The center plane of the DD had an extremely weak magnetic field, with the magnetic field gradient present away from this DD. This magnetic field gradient interacted with the magnetic field, generating the perpendicular current circuit the vicinity of the DD. This current circuit was divided into Earthward and anti-Earthward sides by the DD, and each current circuit flowed between along the DD and the bow shock.

The relationship between the timescale for the complete disruption of accumulated northward IMF in the dayside magnetosheath and the southward IMF parameters was also investigated. It was found that when the velocity, density, and magnetic field strength of the southward IMF were varied, the timescale varied widely, between 5 and 12 minutes. Three major factors were found to change the timescale: (i) fluctuations in the background magnetosheath flow velocity, (ii) changes in the reconnection outflow velocity, and (iii) compression and expansion of the accumulated region due to the dynamic pressure.

Table of contents

List of Figures

List of Table

1. General Introduction

1.1 Geophysical Plasma in the Solar Wind-Magnetosphere-Ionosphere

The space environment surrounding the Earth is comprised of regions with vastly different sizes and properties, such as the solar wind, the magnetosphere, and the ionosphere. The solar wind is a stream of supersonic gas constantly blowing from the Sun. This gas is completely ionized in a state of electrons and ions forming what is known as plasma. Due to the high electrical conductivity, this plasma has the property of confining magnetic fields, thereby dragging the magnetic field from the Sun and releasing it into space as IMFs along with the solar wind. Consequently, the solar wind region consists of particles and magnetic fields originating from the Sun. Solar wind speed is about 400 km/s, it takes several days to reach the Earth. However, the solar wind cannot directly enter the Earth due to the Earth's magnetic field. That is to say, the Earth's magnetic field serves as a barrier, protecting against high-energy particles and radiation from the Sun. This region dominated by the Earth's magnetic field is called the magnetosphere, extending from about 1,000 to 70,000 km in altitude. The supersonic solar wind forms a shock wave front known as the bow shock upon colliding with the Earth's magnetic field, and the solar wind speed decelerates from supersonic to subsonic speeds. On the other hand, the Earth's magnetic fields, originally a tilted dipole structure, are significantly compressed and altered in shape due to the solar wind dynamic pressure. Finally, the ionosphere is the region where Earth's atmosphere becomes separated into ions and electrons due to the effects of solar ultraviolet and X-rays. This region, where low-altitude satellites operate, is approximately 70-1000 km in altitude. Since it is connected to the magnetosphere through magnetic field lines, charged particles accelerated along these field lines interact with the gasses in the ionosphere causing the light. This light is observed as the aurora. Therefore, the aurora phenomenon is a result of solar origin plasma propagating through various regions such as the solar wind, magnetosphere, and ionosphere. To correctly describe the behavior of plasma in space, a kinetic approach based on the Vlasov equation and Maxwell's equations is fundamental. However, the case of the structure and dynamics of Earth's magnetospheric plasma, dealing with large-scale issues in time and space, is frequently described in the MagnetoHydroDynamics (MHD) approximation which treats the plasma as a fluid. Plasma, composed of positively charged ions and negatively charged electrons, can be treated as electrically neutral and uniformly distributed in the solar wind and magnetosphere. The conservation laws in MHD are expressed as follows:

$$\frac{\partial \rho}{\partial t} + \nabla \cdot (\rho v) = 0 \tag{1.1}$$

$$\frac{\partial (\rho v)}{\partial t} + \nabla \cdot \left(\rho v v + pI + \frac{B^2}{2\mu_0} I - \frac{BB}{\mu_0}\right) = 0 \tag{1.2}$$

$$\frac{\partial}{\partial t}\left(\frac{\rho v^2}{2} + \frac{p}{\gamma - 1} + \frac{B^2}{2\mu_0}\right) + \nabla \cdot \left(\frac{\rho v^2}{2} v + \frac{\gamma p v}{\gamma - 1} + \frac{E \times B}{\mu_0}\right) = 0 \tag{1.3}$$

where, $\rho, t, v, p, B, \mu_0, \gamma, and\ E$ are the plasma density, the time, the velocity, the pressure, the magnetic induction, the vacuum permeability, specific heat ratio, and the electric field. Additionally, Ohm’s law and the magnetic induction equation are expressed as follows:

$$E + v \times B = \eta J \tag{1.4}$$

$$\frac{\partial B}{\partial t} = \nabla \times (\mathrm{v} \times \mathrm{B}) + \eta \nabla^2 B \tag{1.5}$$

where, η *and* J are the resistivity and the current. When η equals zero, the condition is referred to as ideal MHD. In ideal MHD, the magnetic field lines and plasma are "frozen-in" to each other, meaning that the magnetic field moves along with the plasma. In the solar wind and the magnetosphere, ideal MHD generally applies. However, if magnetic diffusion terms cannot be ignored, the "frozen-in" condition breaks down, and this leads to magnetic reconnection. Magnetic topology is rearranged, and plasma particles are allowed to transfer to different magnetic field lines. This phenomenon is known as the magnetic reconnection, significant process in plasma physics, that influences various phenomena in the space environment.

1.2 Magnetic Reconnection

Magnetic reconnection is a phenomenon that can alter the magnetic field structure in the magnetosphere. This magnetic reconnection mainly occurs when antiparallel field lines approach each other, and this interaction generates the current sheet between them. The generation process of current can be seen from Maxwell's equation:

$$\nabla \times B = \mu J + \varepsilon\mu \frac{\partial E}{\partial t} \tag{1.6}$$

where, ε *and* μ are the permittivity and the permeability. The second term on the right-hand side of this equation, the displacement current, is possible to generally neglect compared to the first term on the right-hand side. Therefore, magnetic shear generated the current by the first term on the right-hand side. The resistivity of plasma begins to gradually increase by the large current. This large current affects the second term in equation (1.5), the magnetic diffusion term, leading to the occurrence of the magnetic reconnection. In other words, when significant changes in the magnetic field structure, as in the case of the magnetic reconnection, the value of this diffusion term increases, breaking down the "frozen-in" condition of the magnetic field lines.

The structure of the magnetosphere changes depending on the IMF direction, affecting the location and efficiency of the magnetic reconnection. The southward IMF lines are antiparallel to the Earth's closed magnetic field lines at the subsolar point and produce the dayside reconnection (Dungey, 1961). The dayside reconnection creates two open magnetic field lines: one end of which connects to the Earth and the other end extends to the solar wind region. Then, the solar wind flow transports the open magnetic field lines to the Earth's night side across the polar cap. On the other hand, the northward IMF lines reconnect with lobe magnetic field lines at the high-latitude magnetopause (Dungey, 1963; Russell,1972). After the lobe reconnection, two kinds of magnetic field line are generated: one kind does not connect with the Earth, and the other becomes an open field line.

In contrast to this lobe reconnection at the high-latitude magnetopause, the northward IMF lines accumulate in the dayside region because of the absence of an antiparallel magnetic field structure. The characteristic region of the accumulated northward IMF lines in the vicinity of dayside magnetopause is called the "magnetic barrier" (Spreiter & Alksne 1969; Etkaev 1988; Samsonov et al., 2017) or the "plasma depletion layer" (Zwan and Wolf, 1976). In the generated magnetic barrier region, the sum of the magnetic and thermal pressures (= total pressure) increases gradually due to the quickly increasing magnetic pressure while the thermal pressure decreases (Samsonov et al.,2012). This increased magnetic pressure induces a change in the plasma flow direction from earthward to tangential along the magnetic barrier, creating the plasma depletion layer. Bhaskar & Vichare (2013), Ruohoniemi & Greenwald (1998), and Taylor et al (1998) reported from observations that the ionospheric response was delayed by 10-15 minutes when the IMF Direction Discontinuity (DD) from northward to southward arrived. Samsonov et al. (2017) revealed that the cause of this delay was a deceleration in the plasma velocity due to the formation of a magnetic barrier in the vicinity of the dayside magnetopause. This paper also showed that the solar wind plasma crossed the dayside magnetosheath in 3 minutes, but in the case of the DD, it took about 14 minutes. The magnetic barrier was disrupted when the southward IMF lines reached this region and reconnected with the accumulated northward IMF lines. After the IMF reconnection, the magnetic barrier was completely disrupted, and the southward IMF reached the dayside magnetopause (Maynard et al., 2002; Samsonov et al., 2017; 2018). Maynard et al. (2002) predicted the IMF reconnection due to a discontinuous southward IMF turning in the magnetosheath, and reproduced an X magnetic field configuration in 2 minutes associated with arrival of the DD of IMF to the bow shock by using the Integrated Space Weather Prediction Model (ISM). In addition, Phan et al. (2007) and Maynard et al. (2007) used observation data from Cluster and Polar mission, respectively, to confirm the occurrence of the magnetosheath reconnection from the current sheet of the DD. Furthermore, Samsonov et al. (2018) investigated the magnetosheath propagation time of the DD associated with a change in some solar wind parameters by using MHD simulations, spacecraft observation, and analytic calculations. The previous authors concluded that an increase in the solar wind velocity led to a shortness in the magnetosheath propagation time due to a decrease in the magnetic barrier thickness, whereas an enhancement in the IMF magnitude caused a thicker magnetic barrier, thus a longer propagation time. To summarize the previous paper's findings, the northward IMF lines accumulated in the dayside magnetosheath and magnetopause, then formed a magnetic barrier. This accumulation region of northward IMF lines was disrupted via the IMF reconnection after the southward IMF lines reached the bow shock.

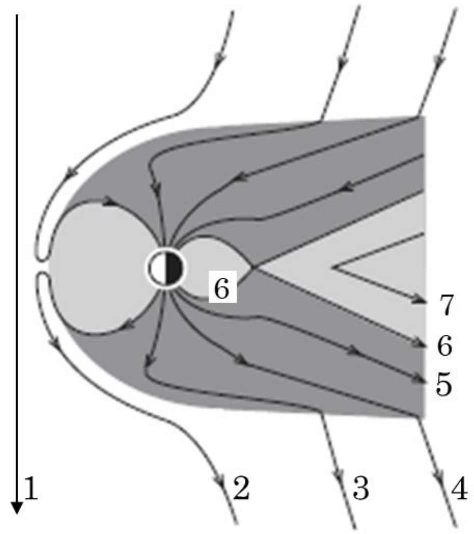

Figure 1.1 Schematic representation of the dayside reconnection, viewed from the dusk side with the Sun to the left. The solid lines represent magnetic field lines, and the arrows on the lines indicate the direction of the magnetic field. Convection is indicated to move 1 to 7 in sequence. This figure is modified by Imber, S. M. et al., (2006).

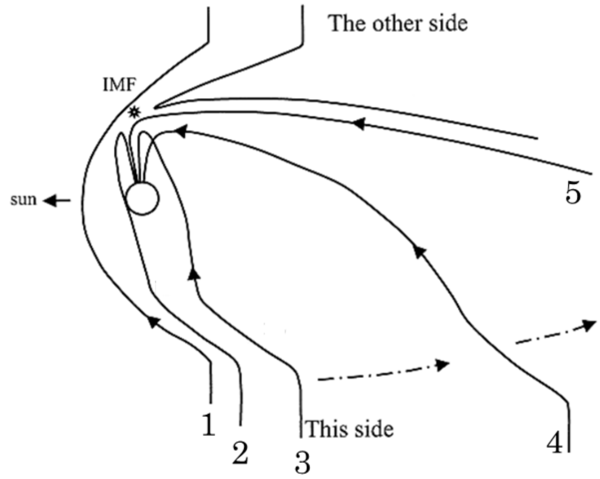

Figure 1.2 Schematic representation of the lobe reconnection, viewed from the dusk side with the Sun to the left. The solid lines represent magnetic field lines, and the arrows on the lines indicate the direction of the magnetic field. Convection is indicated to move 1 to 5 in sequence. This figure is modified by Tanaka et al., (2004).

1.3 Purpose of This Paper

In the field of Solar-Terrestrial Physics, which aims to elucidate phenomena occurring in various regions based on energy from the Sun, the development has been progressing through the comparison of results from three research methods: "theory", "satellite and ground-based observation", and "numerical simulations". The theoretical field is important for clarifying significant physical quantities and systems, thus forming the basis for both observation and simulation. In regard to the observation field, the ionosphere, relatively close to Earth, has become available for three-dimensional observations using ground-based radar and multiple low-altitude satellites. On the other hand, the magnetospheric observation still predominantly relies on single-point observations by a satellite. Therefore, it remains unclear a large part of phenomenon of the magnetosphere.

To progress the research, global simulation has become a powerful method for studying the magnetosphere. With the rapid development of supercomputers and IT infrastructure, numerical simulations, widely used not only in magnetospheric physics but also in meteorology and Earth's internal sciences, can reproduce the entire system as a complex system. This allows us to simulate regions with different sizes and properties, such as the solar wind, magnetosphere, and ionosphere. Numerical simulations also play a crucial role in validating the results of satellite observations. Thus, the "observation" gradually improves accuracy by comparing and verifying its results with simulations, while the "simulation" enhances the understanding of physical phenomena by refining models to align with observational results, mutually influencing each other.

The simulation studying initially requires a quiet magnetospheric state. This is because if the magnetosphere is active states, it becomes difficult to only reproduce the target phenomenon. The activity of the magnetosphere is determined by the amount of energy and plasma particles flowing in from the Sun by the magnetic reconnection. Section 1.2 described how the dayside reconnection and lobe reconnection occur depending on the IMF direction. Generally, the southward IMF is known to result in more injection of energy to Earth. Therefore, in a large part of the numerical simulation research, to create the quiet magnetosphere, the northward IMF has run towards the Earth for about two hours before changing in the IMF parameter for reproduction of the target phenomenon. When the IMF turns to southward, the region where the IMF rapidly changes from northward to southward is formed, and this direction discontinuity(DD) also reaches the Earth. In other words, a large part of the numerical simulation research also has the possibility of effects on the IMF DD. However, the understanding of the plasma and magnetic field structural changes associated with this IMF DD, as well as the quantitative assessment of its effects, remains insufficient. The aim of this thesis is to visualize the effects on the plasma and magnetic field structures as the IMF DD moves from the dayside to the nightside magnetosphere. Furthermore, by comparing these simulation results with satellite observational data, we seek to provide interpretations of these phenomena.

2. Method

2.1 REProduce Plasma Universe (REPPU) code

In this study, we implemented the REProduce Plasma Universe (REPPU) 3D MHD code (Tanaka, 2015). To enhance the resolution of ionospheric grids, this code adopts a system that segments a dodecahedron into a triangular grid structure (Tanaka, 1994). First, this grid system comprised of apexes (20 points) and surface centers (12 points) of a dodecahedron is defined as the primary division and summing up 32 points. Then, each triangle is subdivided into 4 triangles, forming the secondary division. Subsequently, the same operation is repeated to create higher order division (as shown in the Figure 2.1). The number of triangles N on a single spherical surface is given by the following formula.

$$N = 12 \times 5 \times 4^{n-1} \tag{2.1}$$

In this thesis, a grid with a subdivision number of n=6 was used, and eventually, we obtained 61,440 triangles (30,722 grids) in one dodecahedron and stacked 320 dodecahedrons in the radial direction and constructs a 3D coordinate. However, their arrangement is not uniform. For the magnetospheric calculations, it takes on a configuration similar to spherical coordinates around the center, while it becomes cylindrical coordinates in the far distant tail region (as shown in the Figure 2.2). The corresponding modified spherical coordinate elements (r, θ, ϕ) was 320 × 160 × 200, respectively. This unstructured grid structure employed in this model offers a significant advantage over traditional spherical coordinates, as it allows for a grid arrangement without the issue of excessively dense grid structures near the poles, thereby avoiding limitations imposed by the Courant–

Friedrichs–Lewy (CFL) condition. The inner and outer boundaries of the model are set at 2.6 Earth radii (Re) and 200 Re, respectively, and the interval of grids is about 0.5 Re around the subsolar point. Outer boundary conditions are designed to ensure that the gradient of all physical quantities is zero. On the other hand, inner boundary conditions of the magnetosphere, the physical quantities at this location are projected along magnetic field lines to the Earth's radius and connected to an ionosphere model. This connection utilizes the field-aligned current (FAC) injection into the ionosphere. The potential distribution in the ionosphere is calculated based on the FAC and the ionospheric conductivity. Furthermore, the inner boundary for momentum, density, and pressure in the direction from the magnetosphere to the ionosphere are as follows:

$$\frac{\partial(m \cdot n_b)}{\partial l_b} = \frac{\partial \rho}{\partial l_b} = \frac{\partial p}{\partial l_b} = 0 \qquad (2.2)$$

where, $m, n_b, and\ l_b$ are the momentum, the outward unit vector parallel to magnetic field, and the length along n_b.

In this simulation, to reproduce the magnetic reconnection, it is not solving the complete ideal MHD equations throughout the entire regions. This MHD equation includes the magnetic diffusion term, as described in Tanaka et al. (2010). The normalized induction equation is given by:

$$\frac{\partial B'}{\partial t} = \frac{v_0 t_0}{l_0} \nabla' \times (v' \times B') - \nabla' \times \left\{ \left(\frac{\eta t_0}{l_0^2 \mu}\right) \nabla' \times B' \right\} \qquad (2.3)$$

where, $B', v_0\ (= 53.2\ km/s), t_0\ (= l_0/v_0), l_0\ (= 6{,}370\ km), \nabla', and\ v'$ are the normalized magnetic induction, solar wind thermal velocity, transit time, earth radius, normalized nabla operator, and normalized velocity, respectively. The normalized magnetic viscosity is also written as

$$\frac{\eta / l_0 \mu}{v_0} = \nu_m + \nu_r + \nu_n \tag{2.4}$$

where, $\nu_m, \nu_r, and\, \nu_n$ are the normalized model viscosity, normalized reconnection viscosity, and normalized numerical viscosity, respectively. The normalized model viscosity is given by:

$$\nu_m = 0.003 \times \left(\frac{J^2/J_0^2}{B^2/B_0^2 + (0.003)^2} \right) \approx \frac{0.003}{(\Delta l)^2} \tag{2.5}$$

where, $J_0(= 0.0126\, \mu\mathrm{A}/m^2), and\, B_0(= 10\, nT)$ are the normalization units for the current and magnetic induction. Δl is the normalized width of the current sheet. The model viscosity is the most effective in the IMF reconnection. The reconnection viscosity is implicated in the substorm trigger in the magnetic tail. However, in this study, it has little effect because we focused on the dayside region and high latitude magnetosheath. Accurate quantification of the numerical viscosity cannot be estimated, but in our TVD scheme, its value is one order lower compared to the Lax-Wendroff scheme by Ogino et al. (1986). Therefore, the numerical viscosity in our model is assumed to be less significant than the model and reconnection viscosity.

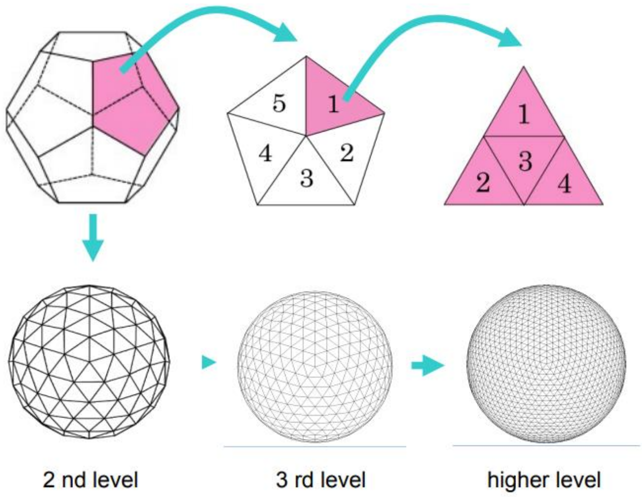

Figure 2.1 Generating a dodecahedral triangular lattice.

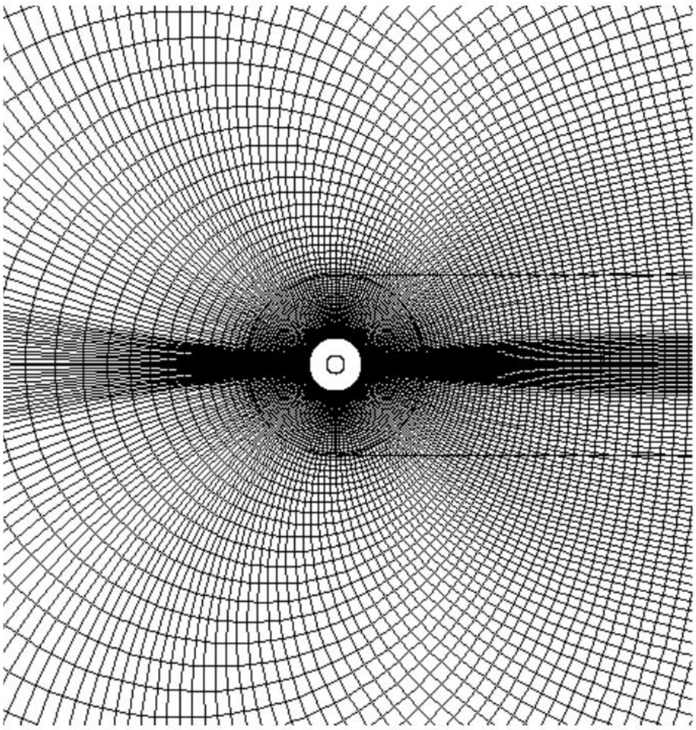

Figure 2.2 An image of the magnetospheric coordinate system in the xz plane. It is spherical near the earth and cylindrical in the down tail. Coordinates in the simulation program is x toward the tail and y toward the dawn side.

3. Effects of IMF Reconnection from Bow Shock to High Latitude Magnetopause

3.1 Description of Simulation

The IMF constantly continuing to blow toward the Earth interacts with the Earth's magnetic field. When the IMF is northward, the reconnection occurs where the antiparallel magnetic field line structure between northward IMF lines and lobe magnetic field lines at the high latitude magnetopause. On the other hand, in the dayside magnetosheath and magnetopause, these field lines are stacked. In particular, it is known to form the magnetic barrier accumulated a large number of northward IMFs in the dayside magnetopause. This magnetic barrier is disrupted when the southward IMF lines newly reach the dayside magnetosheath region and reconnect with the accumulated northward IMF lines due to the antiparallel structure between the northward and southward IMF.

The presence or absence of the magnetic reconnection in this thesis is determined by three physical quantities: the specific magnetic field line structure before and after the reconnection, plasma flow perpendicular to the magnetic field lines ($v_{\perp}$) to confirm the reconnection outflow, and the resistivity. Each physical quantity is explained in detail. First, regarding the specific magnetic field line structure before and after the reconnection, the principle of the magnetic reconnection is already explained in section 1.2., namely a change in the magnetic field line structure due to the generation of the magnetic diffusion. In this study, we assessed the determination of the magnetic reconnection by confirming the presence or absence of the visualization of a change in the magnetic structure. Furthermore, this structure change makes the plasma flow perpendicular to the magnetic field lines dramatically accelerate to the downstream side from the diffusion region due to the expression of Ampère force.

These acceleration flows can be seen in the visualization of the perpendicular plasma flow differed from the surrounding flow speed. Hence, we use the visualization of $v_\perp$ to determine the occurrence of the magnetic reconnection. I this simulation, $v_\perp$ is represented as follows:

$$v_\perp = \frac{1}{B^2}\left[B \times (V \times B)\right] \tag{3.1}$$

$$\mathrm{v}_\perp = \sqrt{(v_\perp)^2} \tag{3.2}$$

where, $\mathrm{v}_\perp$ is the value of the plasma flow velocity perpendicular to the magnetic field.

Finally, the physical interpretation of the resistivity is explained in section 1.2. In the diffusion region where the resistivity is strongly present, the breaking down of the "frozen-in" condition of the magnetic field lines and consequently occurring magnetic reconnection. In the REPPU code, the resistivity primarily inversely proportional to the square of the thickness of the current layer as shown equations (2.4) and (2.5). That is a thinner current layer results in higher the resistivity, and the more occurrence of the magnetic reconnection. Based on the visualization of these three physical quantities, this study determines the presence or absence of the magnetic reconnection.

To obtain a quasi-steady state magnetosphere in our simulation, we first ran 110 minutes under the following conditions: the solar wind density = 5 cm^{-3}, solar wind velocity V_x = 370 km/s, solar wind temperature T = 200,000 K, IMF B_x and B_y = 0 nT and IMF B_z = +5 nT. Then, we changed the IMF B_z from +5nT to -3nT, with the other parameters unchanged. This directional change in the IMF B_z is completed within approximately one minute. While this change appears discontinuous on a large scale, it is continuous under locally over the span of a minute. Observationally, the directional change in B_z also takes at least a minute, making this timescale appropriate for comparison with observational results. The x-axis is oriented towards the Earth, the y-axis is oriented toward the opposite direction of the Earth's orbital motion, and the z-axis is oriented toward the north.

In this study, it is necessary to consider the effects of $B_x = B_y = 0$ nT. When the due northward IMF like $B_x = B_y = 0$ nT flows towards the Earth for a long time, there is a possibility of occurrence dual lobe reconnection. Generally, "lobe reconnection" refers to the reconnection either the Northern or Southern Hemisphere, which is precisely termed as "single lobe reconnection" (Figure 3.1a). In contrast, when the same IMF line reconnects simultaneously with both the north and south lobe magnetic field lines, this type of reconnection is called "dual lobe reconnection" (Figure 3.1b). Dual lobe reconnection results in the formation of closed magnetic field lines at the dayside magnetopause, which moves the magnetopause towards the Sun. However, in this study, the magnetic field line structures associated with dual lobe reconnection, as well as the movement of the magnetopause, were not reproduced in the simulations. Therefore, it is considered that dual lobe reconnection did not occur.

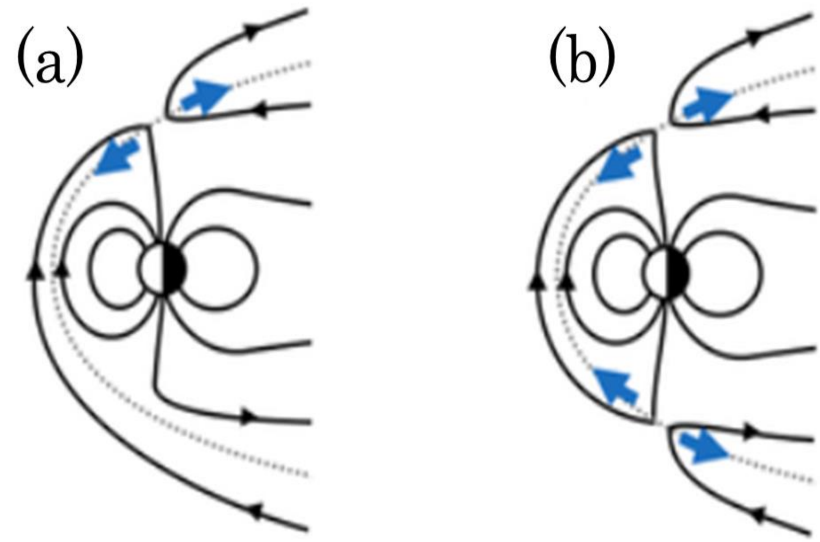

Figure 3.1 Schematic representations of (a) single-lobe reconnection and (b) dual-lobe reconnection. (Milan et al., 2020)

3.2 Simulation Results

3.2.1 IMF Reconnection between Northward IMF and Southward IMF

Figure 3.2 shows the reproduction of the magnetic field lines (black line) and the distribution of the perpendicular plasma flow (contour colors) in the XZ-plane. Here, the time was set to be T = 0 when the southward IMF arrived near the bow shock. Furthermore, the white dots and enclosed areas represent significant resistivity. The central white circle shows the Earth (radius 2.6 Re). In addition, we also discussed the only northern hemisphere due to the nearly symmetrical phenomenon between the southern and northern hemispheres.

The significant plasma flow perpendicular to the magnetic field in the solar wind region was evident because the plasma flow was directed toward the Earth while the IMF was completely southward, causing the two vector fields to be orthogonal. In other words, it was possible to infer the bow shock from a region where the perpendicular plasma flow diminishes because the magnetic field lines inside the bow shock gradually bent.

In Figure3.2, two resistivity regions was marked by white circles. The region occurred in the high latitude magnetopause, was located around +15Re in the z-direction. This resistivity region appeared between the north lobe magnetic field and the northward IMF. The newly merged magnetic field line, whose one end connected to the northern ionosphere and the other extended to the southern solar wind region through the dayside, confirmed the lobe reconnection. This magnetic structure is confirmed by its similarity to the Figure 3.1a. This reconnection was formed by running the simulations for 110 minutes under the northward IMF condition to obtain a quasi-steady state magnetosphere. The lobe reconnection also enhanced the perpendicular plasma flow on the nightside of this reconnection region. However, we note that the visualized fast plasma flow did not necessarily occur the perpendicular flow was strong. Therefore, the presence of visualized perpendicular plasma flow does not necessarily mean that the plasma at that location is moving faster than the surrounding plasma. The strength of the perpendicular plasma flow was affected by the magnetic field structure more than the velocity field so we could not determine the plasma acceleration due to the reconnection. However, it was possible to determine the presence or absence of the reconnection because of the dramatic change in the magnetic configuration.

The other marked resistivity region was near the subsolar point, which appeared between the southward and northward IMF, around -15Re in the x-direction. There was also the significant curvature of the magnetic field line appeared at upside and downside the resistivity region, and both ends of extended to the solar wind region. Since the plasma and magnetic field lines are mainly flowing towards the Earth, the magnetic field lines before the reconnection seem to be the northward and southward IMF. Conversely, the magnetic field lines after reconnection are thought to be those located to the north and south of the resistivity region. We called this reconnected magnetic field lines the “U-shaped magnetic field line”. This reconnection pattern is similar to previous research (Maynard et al., 2007; Samsonov et al., 2017; 2018). In this thesis, we called this magnetic reconnection the “IMF reconnection”. Figure 3.8a shows the typical magnetic field line structure before and after the occurrence of the reconnection including this IMF reconnection. This resistivity region roughly coincides with the bow shock. The magnetic field lines at the right of this resistivity point bend gradually, indicating that this region was located within the magnetosheath. Additionally, focusing on the plasma perpendicular flow in the center of the dayside resistivity region was slightly slower than the surrounding region (Figure 3.2 and 3.3a). The reason behind this slow perpendicular flow was the increase of the x-component of the magnetic field due to the IMF reconnection, since the plasma flow mostly propagated towards the Earth, causing two components to be moderately parallel. Finally, an intermittent structure of the perpendicular flow was produced between the U-shaped magnetic field lines, but this structure will be discussed later.

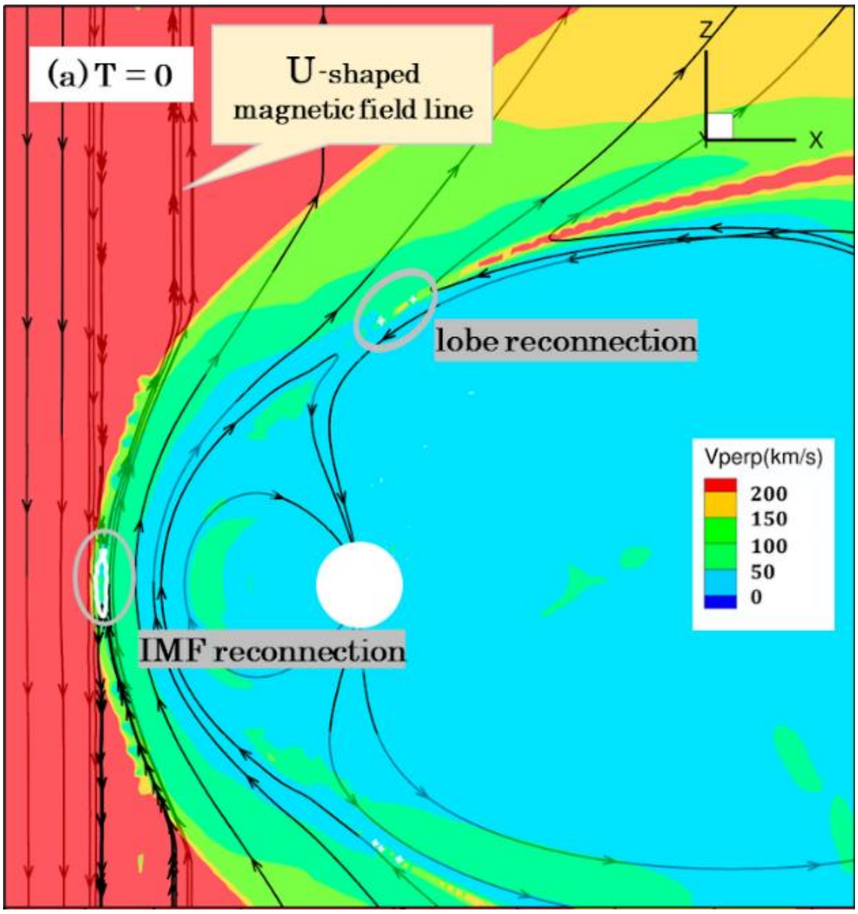

Figure 3.2 The reproduction of the magnetosphere/magnetic field configuration (black lines) and the distribution of the perpendicular plasma flow (contour colors) in the noon-midnight meridian plane. T=0 is the moment when the southward IMF lines reached the bow shock. The X-axis points to Earth, the Y-axis is toward the dusk ward side, and the Z-axis represents the north direction. The central white circle shows the Earth (2.6 Re).

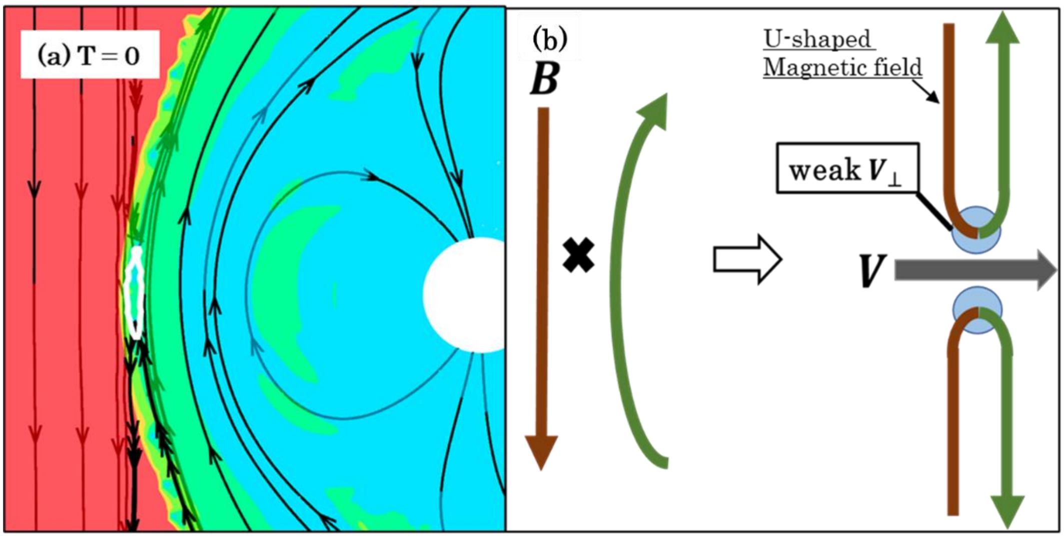

Figure 3.3 Detailed representation of the characteristic distribution of the perpendicular plasma flow. Figure 3.3a shows the same as Figure 3.2. Figure 3.3b shows the schematic for the relationship between the magnetic field lines and the plasma flow.

Figure 3.4 represents the visualization of the perpendicular flow at T=4 minutes after Figure 3.2. The resistivity is visualized in two regions as well. The first region appeared near the lobe reconnection at the high latitude magnetopause, in the same location and shape as in Figure 3.2. On the other hand, the dayside resistivity region moved slightly from the bow shock toward the Earth. This was because the IMF reconnection continuously occurred in the dayside magnetosheath, reducing the accumulated northward IMF. The characteristic existence of the strong and weak perpendicular flows is explained by the relationship between the U-shaped magnetic field line structure and the plasma flow, as shown in Figure 3.5a and 3.5b. That is the curvature of the U-shaped magnetic field lines partially has a structure both parallel and perpendicular to the plasma flow.

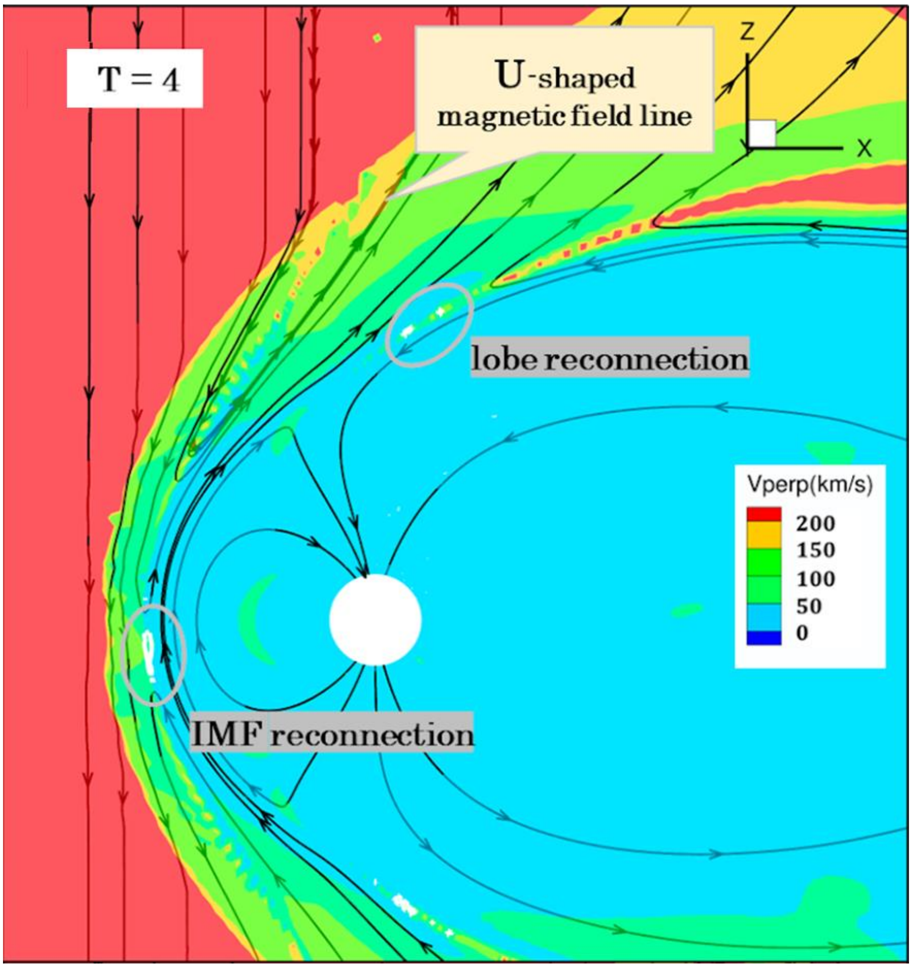

Figure 3.4 The reproduction of the magnetosphere/magnetic field configuration (black lines) and the distribution of the perpendicular plasma flow (contour colors) in the noon-midnight meridian plane (T=4). The X-axis points to Earth, the Y-axis is toward the dusk ward side, and the Z-axis represents the north direction. The central white circle shows the Earth (2.6 Re).

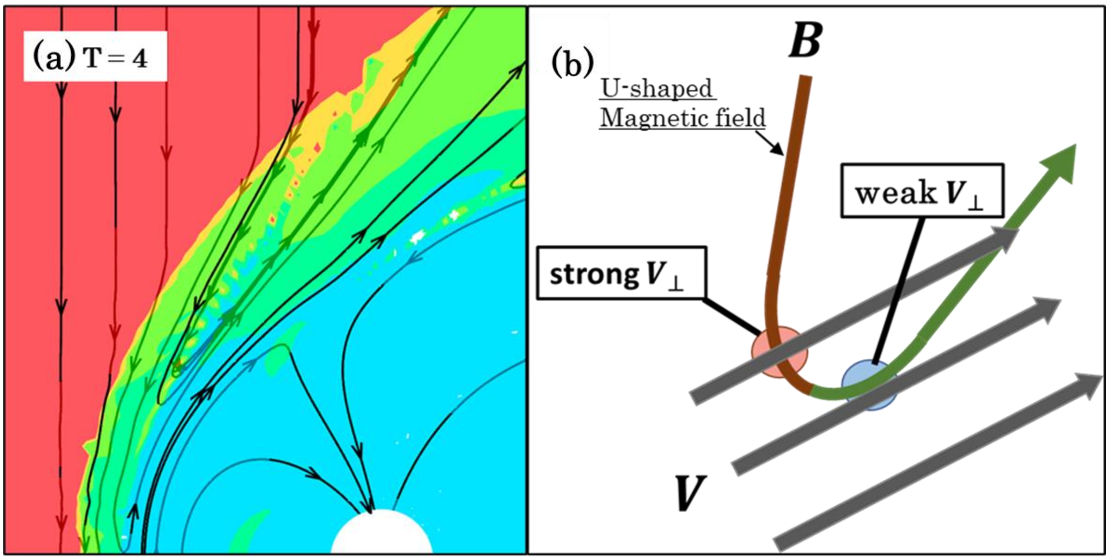

Figure 3.5 Detailed representation of the characteristic distribution of the perpendicular plasma flow. Figure 3.5a shows the same as Figure 3.4. Figure 3.5b shows the schematic for the relationship between the magnetic field lines and the plasma flow.

3.2.2 Reconnection between U-shaped Magnetic Field and Lobe Magnetic Field

Figure 3.6a presents the visualization of perpendicular plasma flow at T=8 after 3.2. The resistivity distribution was similar to Figure 3.2 and 3.4. However, we considered it different from the previous lobe reconnection between the northward IMF and the lobe magnetic field line because of the absence of the northward IMF in Figure 3.6a. In other terms, the accumulation region of the northward IMF in the dayside magnetosheath and magnetopause was completely disrupted due to the IMF reconnection. While the northward IMF involved in the lobe reconnection is no longer present, the structure of the resistivity region and perpendicular plasma flow remain unchanged. Focusing on the magnetic field lines around this resistivity region, the U-shaped magnetic field lines instead of northward IMF were propagated and reached the resistivity region, and then reconnected with a lobe magnetic field line. The newly formed magnetic field line by this reconnection had on a characteristic S shape (Figure 3.6a). In this thesis, we called this magnetic field line the "S-shaped magnetic field line", whose one end connected to the northern ionosphere and the other to the northern solar wind (Figure 3.8b). In the case of the previous lobe reconnection, one end of the reconnected magnetic field lines extended into the southern solar wind from the other end. By comparing a reconnected magnetic field line after the lobe reconnection with the S-shaped magnetic field line, while the reconnection point looked similar, it can be identified as a distinct reconnection phenomenon. In addition, a generation of the S-shaped magnetic field line revealed that the disrupted northward IMF, including the magnetic barrier, which was accumulated in the dayside magnetosheath and magnetopause, connected to the Earth. These results differed from the previous work of Maynard et al., (2002), who suggested that the magnetic field lines reconnected between IMFs propagated tailward without connecting with the magnetosphere.

The visualized magnetic field lines around the dayside resistivity region were southward IMF and closed magnetic field lines. In Figures 3.2 and 3.4, the reconnection in the dayside equatorial region between the northward and southward IMF was known as IMF reconnection. However, as mentioned above, the accumulated northward IMF is no longer present. In Figure 3.6a, the magnetic field line structure surrounding this resistivity region consists of the southward IMF and Earth's closed magnetic field lines, so we proposed that the so-called Dungey-cycle-reconnection took place in this region (c.f. Figure1.1).

The structure of the open magnetic field line after the Dungey-cycle-reconnection closely resembled the S-shaped magnetic field line. The decisive difference between the S-shaped magnetic field line and the magnetic field line after Dungey-cycle-reconnection can be explained by the significant curvature of the S-shaped magnetic field line, even at the high latitude magnetopause (hence appearing as "S-shaped"). Figure 3.6b also represents several magnetic field lines after the Dungey-cycle-reconnection, with no curvature at the high latitude magnetopause, and smoothly connected to the reconnection point.

In Figure 3.6b, the resistivity region was only evident in dayside magnetopause. The Dungey-cycle-reconnection occurred continuously in the dayside magnetopause between the southward IMF line and the closed magnetic field lines. On the other hand, at the high latitude magnetosheath region, the visualized structure of the mixture of the U-shaped, S-shaped, and open magnetic field lines due to Dungey-cycle-reconnection caused a more complex distribution of the perpendicular flow (Figure 3.7 and 3.8c). Subsequently, the U-shaped and S-shaped magnetic field lines propagated towards the night side by the magnetosheath flow, and the anti-sunward convection associated with Dungey-cycle-reconnection gradually became a central process.

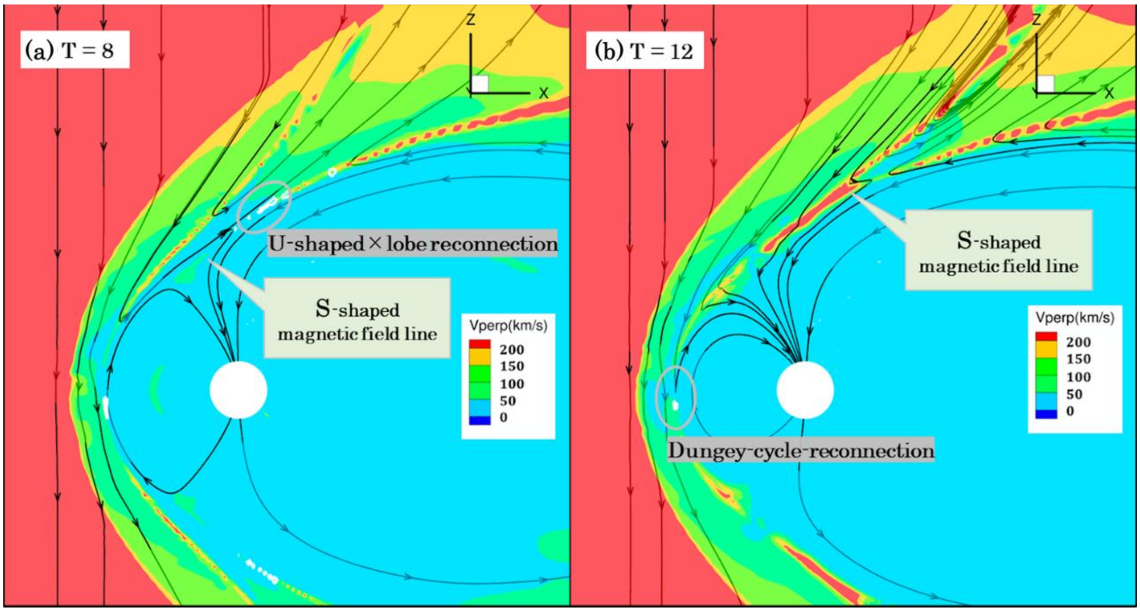

Figure 3.6 The reproduction of the magnetosphere/magnetic field configuration (black lines) and the distribution of the perpendicular plasma flow (contour colors) in the noon-midnight meridian plane at (a)T=8 and (d)T=12. The X-axis points to Earth, the Y-axis is toward the dusk ward side, and the Z-axis represents the north direction. The central white circle shows the Earth (2.6 Re).

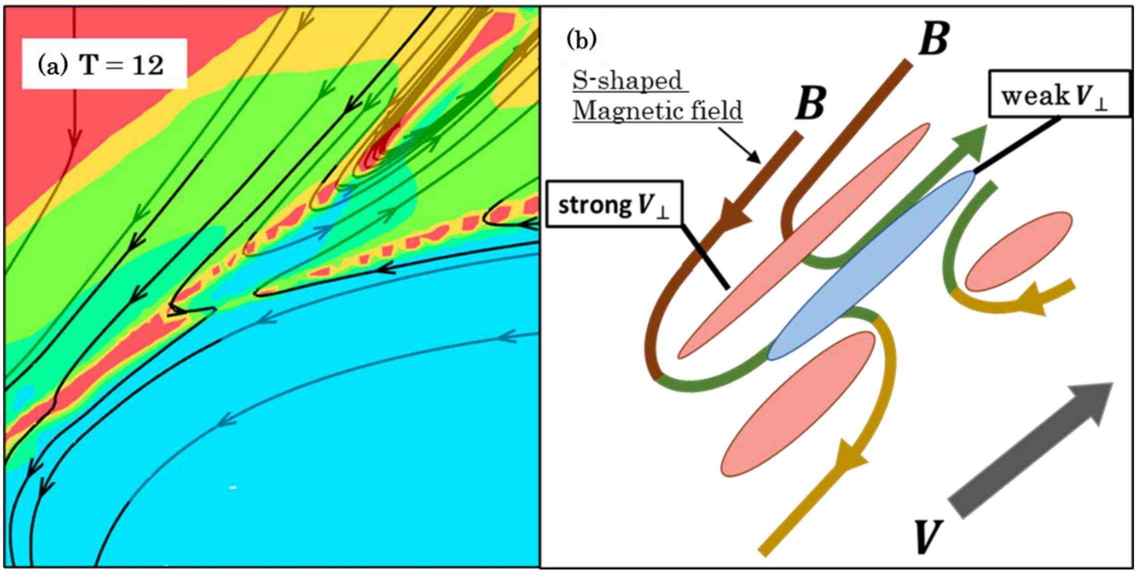

Figure 3.7 Detailed representation of the characteristic distribution of the perpendicular plasma flow. Figure 3.7a shows the same as Figure 3.6b. Figure 3.7b shows the schematic for the relationship between the magnetic field lines and the plasma flow.

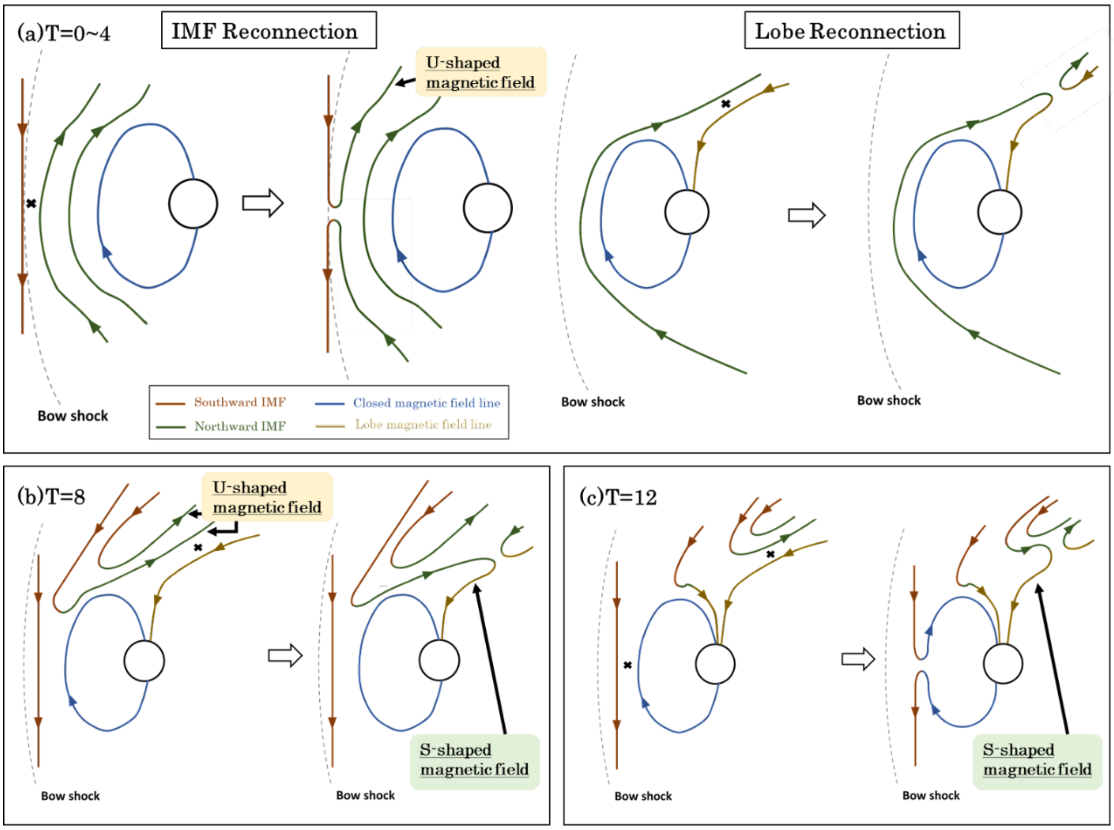

Figure 3.8 Schematic for a change in the magnetic field lines before and after the occurrence of the reconnection, viewed from the dusk side with the Sun to the left. Visualized situation at (a)T=0-4 min, (b)T=8 min, and (c)T=12 min, respectively. The line represents the origin of the magnetic field line: southward IMF (red); northward IMF (green); closed field line (blue); and lobe magnetic field line (ocher), respectively.

3.3 Discussion

3.3.1 Disruption of Accumulated Northward IMF Lines

This study demonstrated the effect of the IMF direction change from the due northward to due southward. In order to establish an initial magnetosheath state, we ran our simulations for 110 minutes under the northward IMF condition. After their accumulation between the bow shock and magnetopause, the IMF reconnection occurred when the southward IMF lines reached the bow shock. It is widely recognized that the dayside reconnection is called the Dungey-cycle-reconnection, but in the present result, reconnection was different. This was because there was evidence that a southward IMF line did not reconnect with the closed magnetic field lines but with the northward IMF. Similarly, the presence of a U-shaped magnetic field line, produced by this IMF reconnection between northward and southward IMFs, also confirms the difference between this IMF reconnection and the Dungey-cycle-reconnection (Figure 3.8a). In the case of the Dungey-cycle reconnection, the open magnetic field lines, whose ends connected to the Earth and the others extended to the solar wind region, should be created. First, the northward IMF decelerated in front of the southward IMF during the process across the bow shock, then the following southward IMF caught up, resulting in the IMF reconnection process. Maynard et al. (2002) obtained the X-type configuration within 2 minutes when the IMF directional discontinuity initially contacted the bow shock. The previous work supported our study findings in demonstrating the rapid commencement of the reconnection process. Inside the bow shock, the northward IMF lines were abundant, especially near the magnetopause, where they accumulated and formed the so-called "magnetic barrier" (Spreiter & Alksne 1969; Etkaev 1988; Samsonov et al., 2017). This IMF reconnection continuously reduced the number of accumulated northward IMF lines from the bow shock to the magnetopause until the magnetic barrier region was completely disrupted. Figure 3.4 shows the disruption process of the accumulated northward IMF lines. Here, we provided the possibility that the lobe reconnection reduced the magnetic barrier thickness as well as the IMF reconnection. In Figure 3.2 and 3.4, this lobe reconnection between the lobe magnetic field line and the northward IMF line continuously occurred. This northward IMF line involved in the lobe reconnection can be considered as a part of the magnetic barrier region. Hence, we may assert that this lobe reconnection disrupted the magnetic barrier region. Based on the previous discussion, the disruption of the magnetic barrier region can be explained by two reconnection patterns: One reconnection was the IMF reconnection starting from the bow shock, and the second was the lobe reconnection at high latitude magnetopause.

Finally, we discuss the slight southward shift of the IMF reconnection point as the IMF DD approaches the dayside magnetopause. In Figures 3.4 and 3.6, the significant resistivity region and the source of the U-shaped magnetic field are located slightly south of the equatorial plane, namely indicating a southward movement of the IMF reconnection point. In this simulation, the IMF input parameters were the due northward and southward IMF, and the Earth's magnetic field employed the dipole geomagnetic field, so it is difficult to be produced the asymmetric structure. Here, we propose that this asymmetry was caused by interchange reconnection, first suggested by Tanaka (1999). This reconnection is characterized by the interchanging of topologies of two magnetic field lines before and after the reconnection. In Figure 3.9a, the northward IMF and the lobe magnetic field occur the interchange reconnection, resulting in the interchange in topologies each other. Subsequently, as shown in Figure 3.9b, the newly formed lobe magnetic field labeled 2' occurs the interchange reconnection with the nightside's closed magnetic field, then creating the closed magnetic field on the dayside and the lobe magnetic field labeled 4 on the nightside. This nightside lobe magnetic field labeled 4 is used in the interchange reconnection again as the lobe magnetic field labeled 4' in this figure3.9a. These frameworks are called the interchange cycle. It is important to note that the interchange reconnection at the northern and southern hemisphere high latitude magnetopause does not occur simultaneously. If the reconnection occurred simultaneously there, it was called the dual lobe reconnection (as shown in Figure 3.1b). While we might expect the occurrence of the dual lobe reconnection under the due northward IMF, it was actually the interchange reconnection took place (Tanaka et al., 2019). We believe that the timing differences of the interchange reconnection occurrence between the northern and southern hemisphere contribute to asymmetry magnetic field structure in the dayside magnetosheath and magnetopause. Even a slight precedence in the occurrence of the first IMF-to-lobe reconnection in one hemisphere leads to the fast reconnection outflow (detailed in section 4.1), which then starts to significantly alter the surrounding magnetic field line structure. This asymmetrical magnetic field structure may lead to the southward movement of the reconnection point.

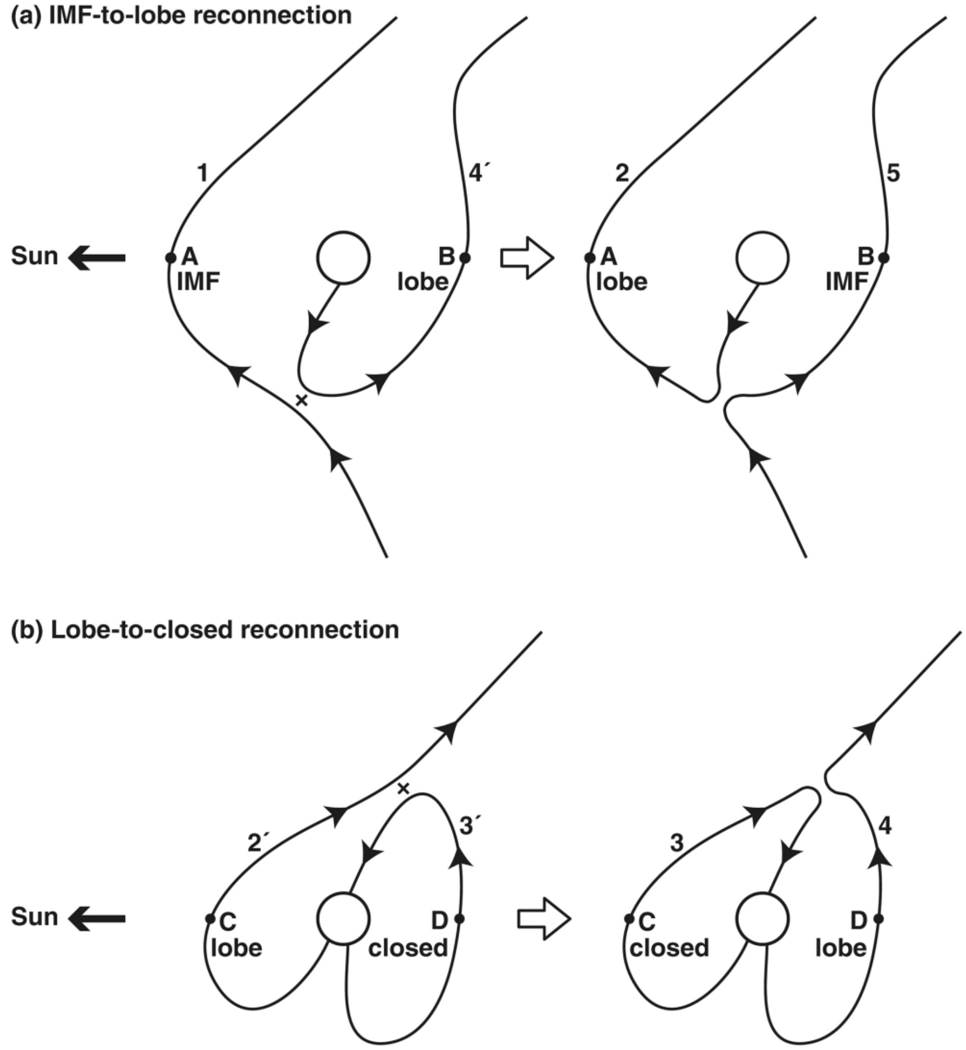

Figure 3.9 Schematic for the interchange cycle in the case of the IMF first contacting with the south lobe (taken from Watanabe et al., 2018)

4. Characteristics of IMF Reconnection

4.1 Magnetic Reconnection Outflow

The magnetic reconnection mainly occurs when antiparallel field lines firstly approach each other, and this interaction generates the current sheet between them. The resistivity region develops in the plasma due to the large-scale current, the "frozen-in" condition breaks down, leading to the magnetic diffusion and the reconfiguration of magnetic field lines (c.f. section 1.2).

The plasma flow entering or exhausting the diffusion region is known as the inflow or outflow. Reconnected magnetic field lines have the significant magnetic tension that accelerates the plasma and forms a fast outflow. If we assume that the pressure difference between the inner current sheet pressure (p_i) and the outer current sheet pressure (p_o) accelerates the outflow, the velocity can be determined as follows:

$$p_i - p_o = \frac{1}{2}\rho v_0^2 \qquad (4.1)$$

The magnetic pressure is zero at the center of the current sheet, so the pressure balance of the plasma can be expressed as follows:

$$p_i - p_o = \frac{B_0^2}{2\mu_0} \qquad (4.2)$$

(4.1) and (4.2) equations give the following equation,

$$\frac{1}{2}\rho v_0^2 = \frac{B_0^2}{2\mu_0} \tag{4.3}$$

$$v_0 = \frac{B_0}{(\mu_0\rho)^{1/2}} \equiv v_A \tag{4.4}$$

where, v_A is the Alfvén velocity. (4,4) equation shows the outflow velocity corresponds to the Alfvén velocity.

4.2 Plasma Flow of Simulation Results

4.2.1 Plasma Velocity toward Z-component

In the section 3.2, we demonstrated the occurrence of IMF reconnection between northward and southward IMF, which had not been detailed in previous studies. However, in Figure 3.2 and 3.4, the perpendicular plasma flow significantly varied depending on the local magnetic field structure. This was not able to confirm the accelerated reconnection outflow associated with the IMF reconnection. It is believed that the magnetic tension after the IMF reconnection predominantly points in the Z direction, so the appearance of the outflow is predicted the same direction (Figure 4.1). Therefore, the visualization of the Z component of plasma velocity (V_z) is necessary to confirm the formation of this accelerated outflow. Figure 4.2 shows the magnetic field lines (black lines) and the distribution of the Z component of the plasma velocity (contour colors) at T=0 and 4. Figure 4.1a, the moment when the southward IMF lines reached the bow shock, has no notable changes in V_z between the U-shaped magnetic field lines because the magnetic tension has not yet sufficiently influenced the plasma acceleration. On the other hand. Figure 4.1b at T=4 shows a significant elapsed time since the start of the IMF reconnection. The reconnection diffusion region was almost at the subsolar point (Figure 3.4), and it is evident that the V_z between U-shaped magnetic field lines is about 20 km/s faster than the surrounding velocity. This difference occurs likely between the U-shaped magnetic field lines because the magnetic tension is most effective there. The slightly Earthward shift of the reconnection outflow is due to the composition of velocities with the magnetosheath flow, which primarily flows Earthward.

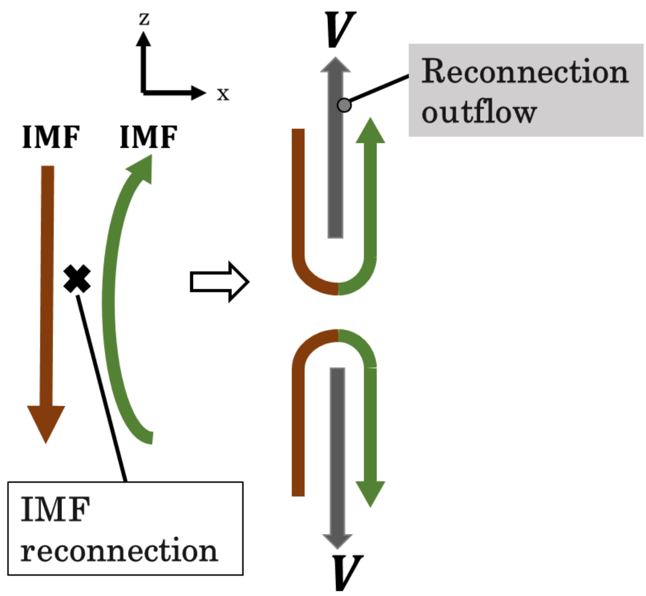

Figure 4.1 Schematic for the direction of the IMF reconnection outflow

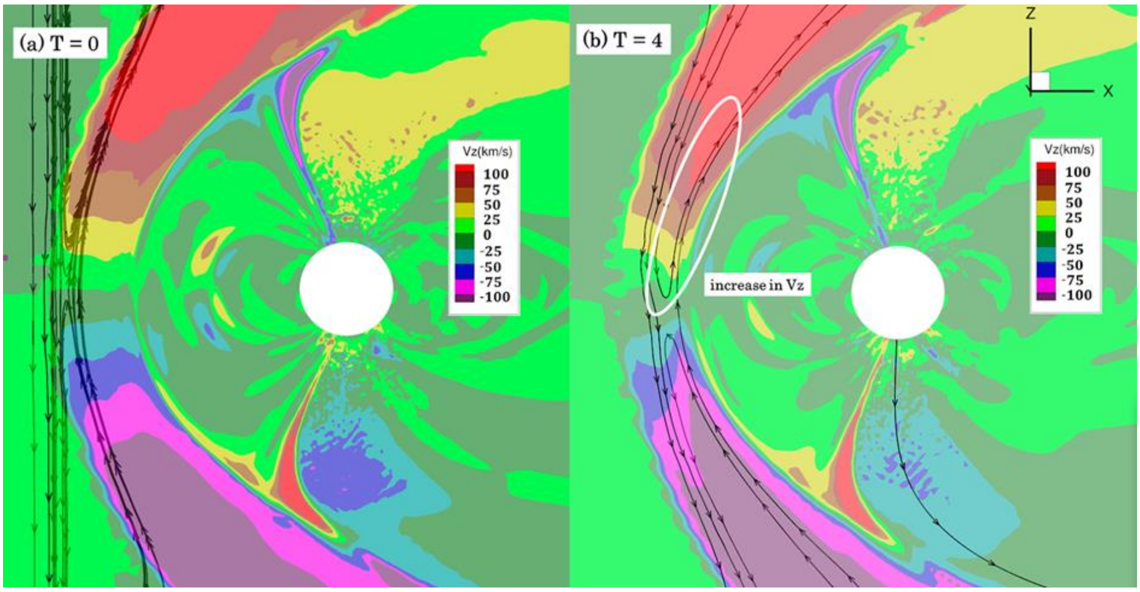

Figure 4.2 The reproduction of the magnetic field configuration (black lines) and the distribution of the Z component of plasma velocity (contour colors) in the noon-midnight meridian plane (a) T=0 and (d) T=4. The X-axis points to Earth, the Y-axis is toward the dusk ward side, and the Z-axis represents the north direction. The central white circle shows the Earth (2.6 Re).

4.2.2 Plasma velocity Perpendicular to the Magnetic Field

So far, we revealed the occurrence of the IMF reconnection and the formation of the reconnection outflow by using the V_z and perpendicular plasma velocity. Additionally, we discuss the Z component of the perpendicular plasma flow (V_{perpz}). The visualization of the V_{perpz} was conducted by the Z component from the equation (3.1). As a result of the IMF reconnection, reconnected magnetic field lines had an X component, while the reconnection outflow associated with the magnetic tension was oriented in the z-direction (c.f. Figure 4.1). Therefore, the V_{perpz} has the significant velocity. In Figure 3.2 and 3.4, the X component of the perpendicular plasma flow was the dominant value within the solar wind region due to the plasma flow and the IMF direction were completely orthogonal. This large value probably effects on the color range of some Figure. By excluding these components, the characteristic of the IMF reconnection can more accurately be represented. Figure 4.3a shows the visualization of the V_{perpz} at T=0. We found an intermittent $V_{\perp z}$ distribution marked between the U-shaped magnetitic field lines. A similar structure also appears in Figure 3.2. Here, to clarify whether this intermittent $V_{\perp z}$ structure formed only the IMF reconnection, we visualized $V_{\perp z}$ during Dungey-cycle-reconnection, as shown in Figure 4.3b. The structure of the Dungey-cycle-reconnection in the dayside magnetopause was not intermittent but rather continuous. Based on these results, we revealed a unique intermittent $V_{\perp z}$ structure appearing only in the IMF reconnection.

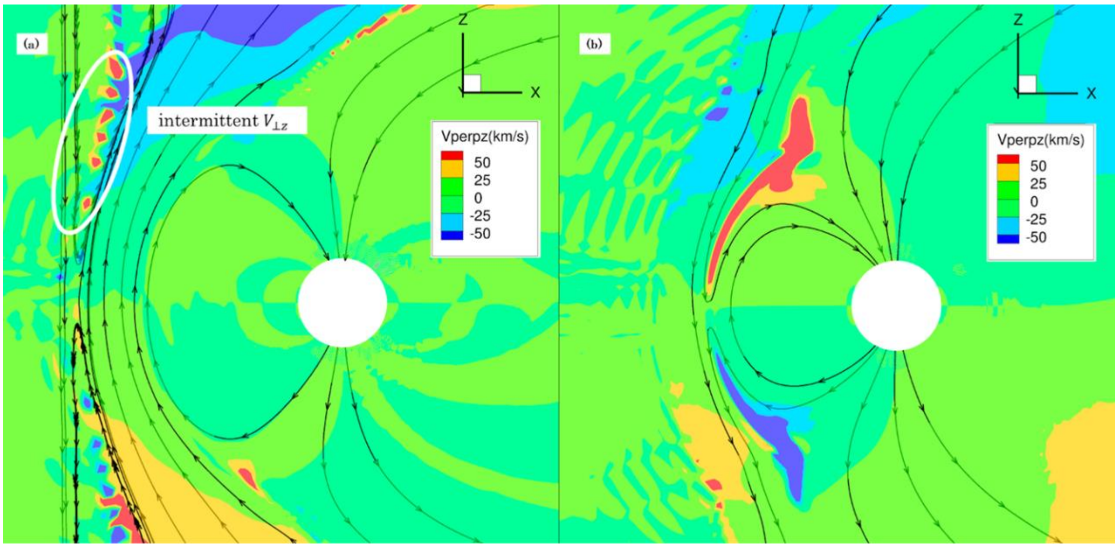

Figure 4.3 The reproduction of the magnetic field configuration (black lines) and the distribution of the z-component of perpendicular plasma flow (contour colors) in the noon-midnight meridian plane. Panel a represents the situation when the southward IMF lines reached the bow shock (T=0). Panel b is the situation after the southward IMF lines reached the dayside magnetopause following an extended simulation period.

4.3 Plasma Flow of Observation Result by Geotail

In this thesis, we confirmed the IMF reconnection outflow velocity by GEOTAIL observations. During the time interval, 4 May 2013 15:24:00 — 15:25:00UT, GEOTAIL observed a change in the IMF B_z component from +20nT to -20nT at XGSM = 11.35 Re, YGSM = 4.44 Re, and ZGSM = 2.29 Re in Figure 4.4. The plasma velocity toward the Z-direction accelerated, by approximately +75km/s, in response to the arrival of the southward turning of the IMF. These changes might be a consequence of the U-shaped magnetic field passing through the Geotail. In other words, a significant possibility, an IMF reconnection occurred and observed these effects in this event, was evidenced by the fact of the observation both the shift in the IMF direction from northward to southward and the accelerated plasma outflow at that same time. In Figure 4.2b, V_z increased by 20 km/s faster between the U-shaped magnetic field lines relative to the background magnetosheath flow velocity in the exhaust direction from the IMF reconnection point. It was difficult to find a situation when a southward IMF turning reached the spacecraft position in the dayside magnetosheath. However, there was a significant possibility that an IMF reconnection occurred in this event.

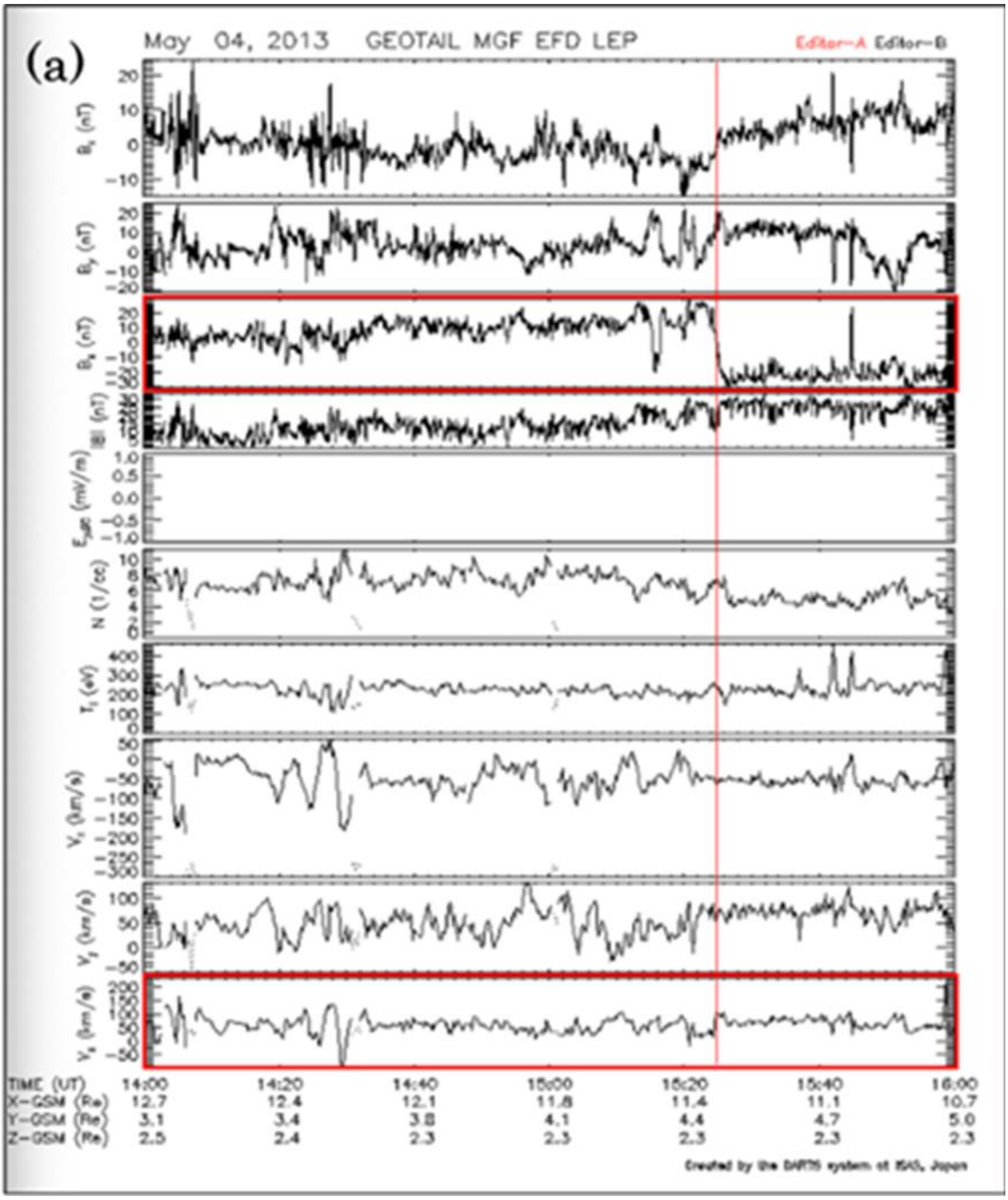

Figure 4.4 The figure visualizes the IMF reconnection outflow from GEOTAIL and simulations. The IMF observed by GEOTAIL in the dayside magnetosheath. The vertical red line marks the selected southward turning during the time interval, 15:24:00—15:25:00 on 4 May 2013.

4.4 Discussion

4.4.1 Compared with Other Reconnection Flow

The magnetic reconnection is generally known to be accompanied by the reconnection outflow, with increasing the velocity in the outward direction from the X magnetic field region. For instance, such configuration appears regarding to reconnection in the nightside plasma sheet that triggers a substorm, Eriksson et al. (2020) observed a reconnection jet with an ion velocity (V_i) of around 1000 km/s using the MMS satellites. Fujimoto et al. (1996) observed a tailward jet (1600 km/s) by GEOTAIL, and simulations reproduced similar characteristics. Koga et al. (2019) selected 25 dayside magnetopause reconnection events using the THEMIS satellite observations (see Table 1), and the median outflow speed was approximately 200 km/s.

Both in the observations and simulations related to this research, the IMF reconnection accelerated the plasma up to about 20 to 75 km/s. However, this acceleration appeared to be slow as compared with the accelerated reconnection outflow in the nightside plasma sheet or the dayside magnetopause. Generally, the theoretical outflow speed is proportional to the Alfvén speed based on the upstream magnetic fields and density (Cassak & Shay, 2007; Birn et al., 2010). Here, this IMF reconnection occurred from the bow shock to the dayside magnetosheath, where the upstream magnetic field strength was substantially weaker than the nightside plasma sheet and the dayside magnetopause. This occurred because, as one moves farther from Earth, the accumulation of the magnetic field decreases, resulting in reduced magnetic pressure. Therefore, we considered that this weak magnetic field led to a decelerated IMF reconnection outflow.

4.4.2 IMF Reconnection Frequency

In this section, we will explain the reason for this intermittent structure attributed to the deceleration of the IMF reconnection outflow. The IMF reconnection between the accumulated northward and southward IMF lines, transformed the magnetic field lines into the U-shaped magnetic field lines, and then carried them downstream by the magnetic tension. However, in the case of the IMF reconnection, where the outflow was slow, the U-shaped magnetic field lines did not move downstream effectively. The U-shaped magnetic field must move a certain distance downstream from the diffusion region before the next IMF reconnection can occur, as shown in Figure 4.5. Consequently, the frequency of IMF reconnection events becomes considerably low. The U-shaped magnetic fields generated with each occurrence of IMF reconnection are intermittently sent downstream. This results in the formation of the characteristic intermittent V_{perpz} structure between the U-shaped magnetic field lines, as depicted in Figure 4.6.

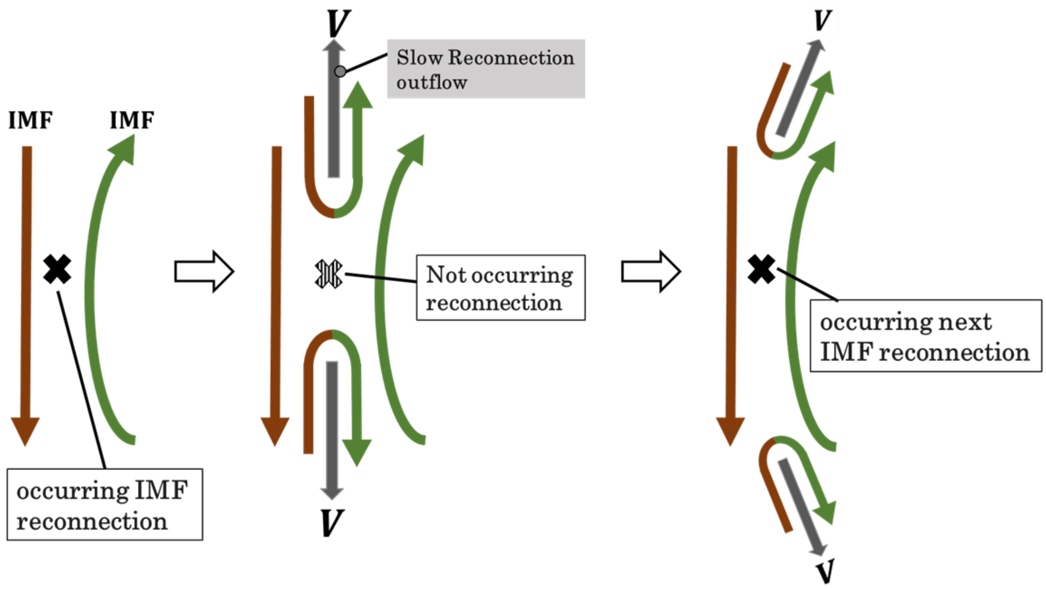

Figure 4.5 Schematic for the continuous occurrence of the IMF reconnection

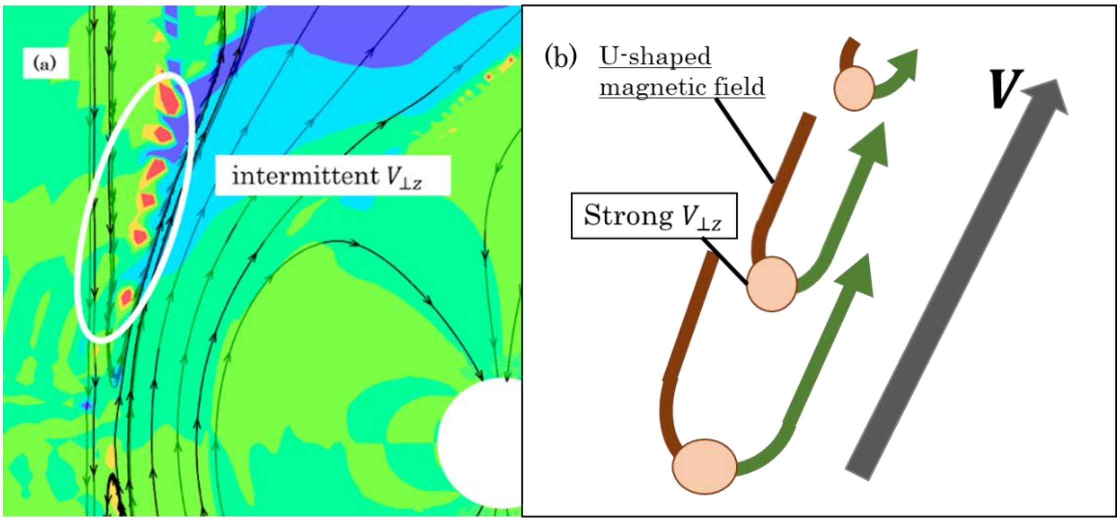

Figure 4.6 (a) Detailed representation of the characteristic distribution of the Z component of the perpendicular plasma flow. Figure 4.6a shows the same as Figure 4.3a. (b) Schematic for the relationship between the magnetic field lines and the plasma flow.

5. Characteristic of Direction Discontinuity

5.1 Distribution of Magnetic Field Strength

In this thesis, we initially ran 110 minutes under the northward IMF toward the Earth, and then we switched to the southward IMF. The magnetic field strength was +5nT and −3nT, respectively. These directional changes in the IMF B_z appears discontinuous on a large scale. However, in reality, these changes occurred smoothly over a short time. Specifically, in this simulation, there was a distance of about 7 Re when the magnetic field strength changes from +5nT to -3nT within approximately one minute, as shown in Figure 5.1. Moreover, observational data also indicated similar time scales for the IMF direction discontinuity with changes within one minute, as shown Figure 4.4. Within the process of the changing magnetic field direction, there is a possibility to form a significantly weaker magnetic field strength region at the center plane of the discontinuity. Figure 5.2, the magnetic field strength at T=4, reproduced the weaker magnetic field strength region compared to surrounding regions. On the other hand, IMF reconnection occurs within the center of DD, where the magnetic field strength is markedly weak.

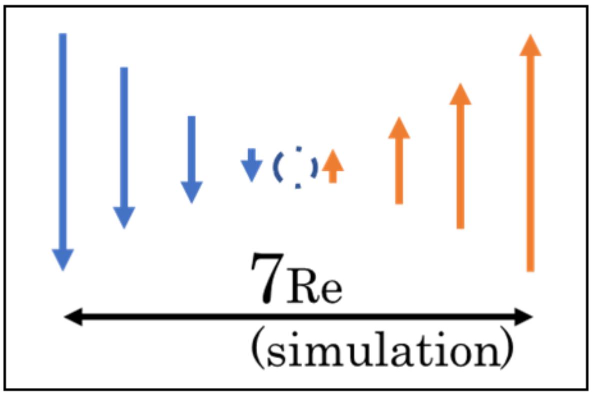

Figure 5.1 Schematic for a discontinuous change in the magnetic field lines

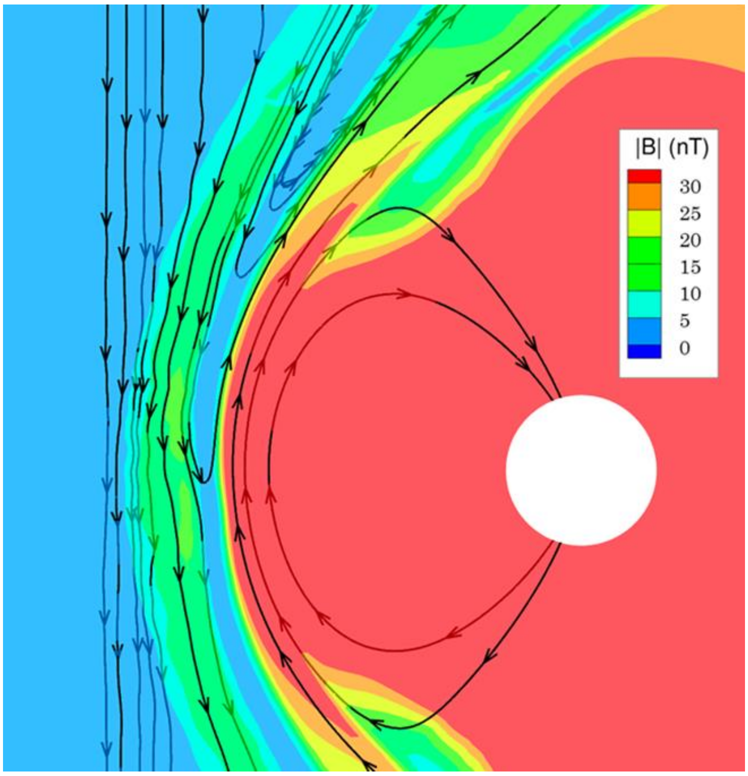

Figure 5.2 The reproduction of the magnetosphere/magnetic field configuration (black lines) and the distribution of the magnetic field strength (contour colors) in the noon-midnight meridian plane (T=4). The X-axis points to Earth, the Y-axis is toward the dusk ward side, and the Z-axis represents the north direction. The central white circle shows the Earth (2.6 Re).

5.2 Effects of Weak Magnetic Field Strength at Center of DD

Figure 5.3 represents the distribution of a current structure perpendicular to the magnetic field. The mechanism for the magnetic reconnection had been discussed in section 1.2. The current was generated by the Ampère's low between anti-parallel magnetic field lines, initiating the diffusion of the magnetic field. This structure persists even after the magnetic reconnection occurs due to the significant magnetic curvature. This perpendicular current can be expressed in terms of Ampère's force, is given by

$$J \times B = \frac{B^2}{\mu}\left(-\frac{\nabla B}{B} + (b \cdot \nabla)b\right) \tag{5.1}$$

where, b is the unit vector of the magnetic field. The first term on the left-hand side shows the magnetic pressure force and the right-hand side shows the magnetic tension force. By taking the curl of B with this equation,

$$B \times (J \times B) = \frac{B^2}{\mu}\left(-\frac{\mathrm{B} \times \nabla B}{B} + B \times (b \cdot \nabla)b\right) \tag{5.2}$$

$$J_\perp = \frac{1}{\mu}\left(-\frac{\mathrm{B} \times \nabla B}{B} + B \times (b \cdot \nabla)b\right) \tag{5.3}$$

where, $J_\perp$ is the current perpendicular to the magnetic field. Before and after the reconnection, the perpendicular current is expected to be generated between U-shaped magnetic field lines due to the second term on the right-hand side in equation (5.3). However, in Figure 5.3, we cannot find this current structure there. Instead, the current structure is observed on the Earth's side, as well as the anti-Earth's side slightly.

The reason why the absent perpendicular current between the U-shaped magnetic fields can be attributed to the magnetic field strength in this region, nearly 0nT, as demonstrated in section 5.1. The magnetic field strength close to 0nT means that both the first and second terms on the right-hand side of equation (5.3) do not attain significant values.

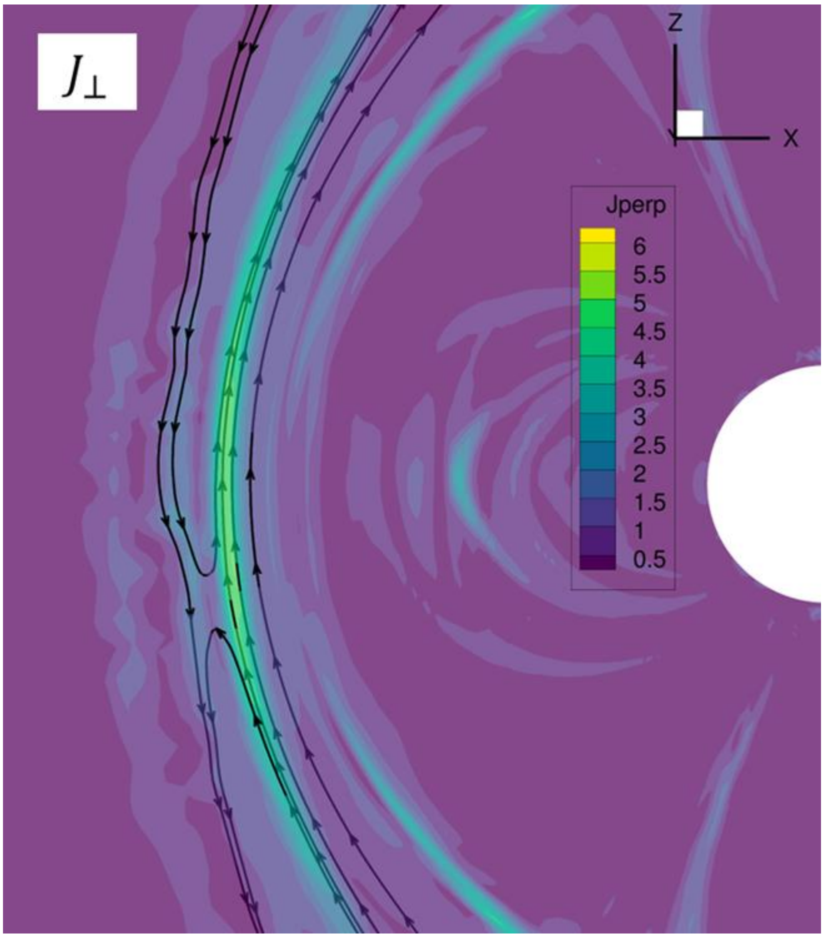

Figure 5.3 The reproduction of the magnetosphere/magnetic field configuration (black lines) and the distribution of the current perpendicular to the magnetic field (contour colors) in the noon-midnight meridian plane (T=4). The X-axis points to Earth, the Y-axis is toward the dusk ward side, and the Z-axis represents the north direction. The central white circle shows the Earth (2.6 Re).

5.2.1 Magnetic Tension

In section 5.1, simulation results showed that the magnetic field is extremely weak between the IMF DD. This weak magnetic field induced the minimal development of the perpendicular current, even when anti-parallel magnetic field lines approached each other.

Considering a very weak magnetic field state in equation (5.1), if B is nearly 0nT, it can be expected that the Ampère's force (i.e., $J \times B$) will not be activated. This implies that the vicinity of center the IMF DD, where IMF reconnection occurs, the Ampère's force based on this reconnection might not develop. This fact significantly affects the generation process of the reconnection outflow. In section 4, it was shown that the magnetic tension, one component of Ampère's force, accelerates the plasma to downstream side, and the creation of the reconnection outflow. This outflow was revealed both in simulations and an observation's result. Therefore, the visualization of the magnitude of Z-component of the magnetic tension was conducted, was given by Figure 5.4. It revealed the strong magnetic tension between the IMF DD, or in other words, the U-shaped magnetic field lines. Although the magnetic field was very weak, the magnetic shear is significantly larger than the surroundings. This shear effects negates the effect of the weak magnetic field. Thus, the occurrence of the IMF reconnection outflow due to the magnetic tension can be coherently explained.

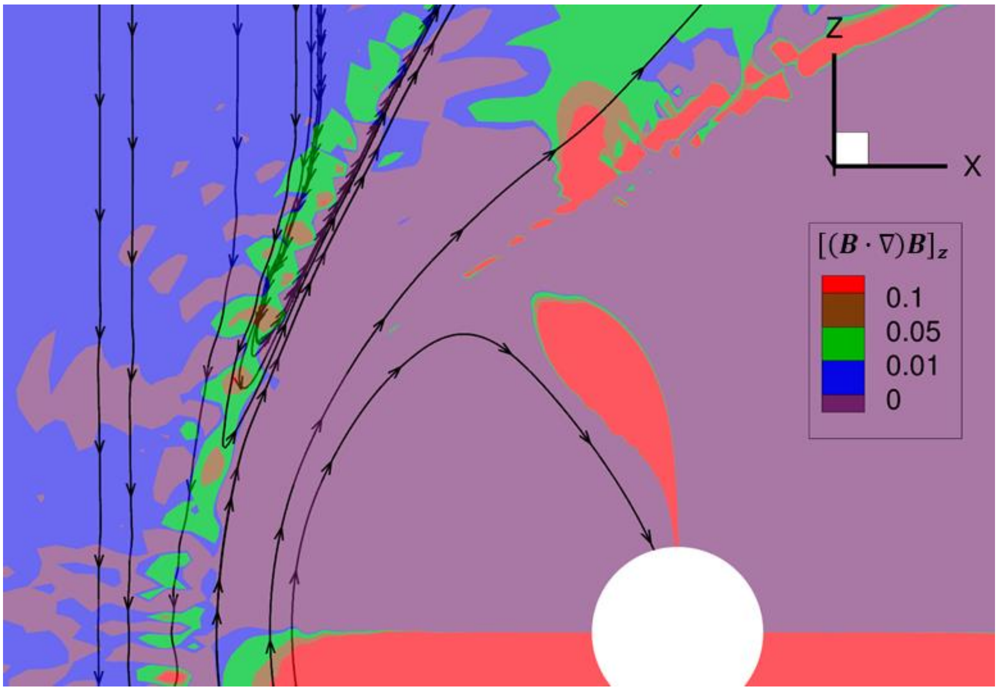

Figure 5.4 The reproduction of the magnetosphere/magnetic field configuration (black lines) and the distribution of the magnitude of Z-component of the magnetic tension (contour colors) in the noon-midnight meridian plane (T=4). The X-axis points to Earth, the Y-axis is toward the dusk ward side, and the Z-axis represents the north direction. The central white circle shows the Earth (2.6 Re).

5.2.2 Magnetic Pressure

In section 5.2.1, the impact of the second term on the right-hand side of equation (5.1) was discussed. Here, we will discuss the magnetic pressure, the first term on the right-hand side of equation 5.1, and its relation to the DD. As clearly shown in Figure 5.2, the center of the IMF DD, where the IMF reconnection occurs, has the very weak magnetic field. However, the magnetic field attains moderate values away from the center of the IMF DD in the X direction. This implies that there are the magnetic gradients in both the Earthward and anti-Earthward from the center of the IMF DD. In addition, Figure 5.2 reveals that these gradients are not symmetrical in both directions; the gradient towards the Earth is overwhelmingly larger due to the large number of accumulated magnetic field lines closer to Earth (Figure 5.5). Considering moderate magnetic field away from the center of DD, the first term on the right-hand side of equation (5.1) and the first term on the right-hand side of equation (5.3) have some values. Therefore, the development of the Jperp in the regions away from the DD, as observed in Figure 5.3.

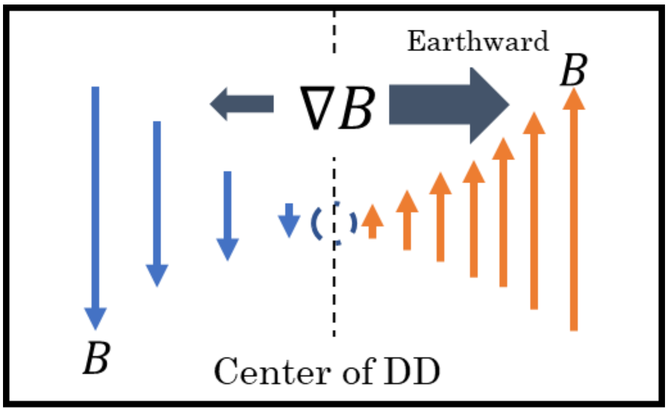

Figure 5.5 Schematic for a magnetic gradient from the DD

5.3 Current Circuit around DD

In section 5.2, it was established that the perpendicular current was generated due to the magnetic field gradient in regions slightly away from the center of the IMF DD, so we will consider this perpendicular current circuit. With respect to the first term on the right-hand side in equation (5.3), since magnetic field lines primarily have a Z-component because of an input IMF direction under due northward or southward and the gradient of the magnetic field is dominated by the X-component, their cross product results in J_{perp} having a value in the Y direction. Figure 5.6 visualizes the distribution of the Y-component of the current perpendicular to the magnetic field line. In this figure, it becomes apparent that the Y-component of the Jperp flows towards the dusk side on both the Earthward and anti-Earthward sides of the DD. Both sides point towards the dusk side, when the northward IMF takes the curl of the Earthward magnetic field gradient on the Earthward side, and the southward IMF takes the curl of the anti-Earthward magnetic field gradient on the anti-Earthward side. The next section will discuss each of these current circuits using the results from simulations.

Next, we discuss the current circuit flowing away from the anti-Earthward side of the DD. Figure 5.7 shows the current perpendicular to the magnetic field (line) and the distribution of (a) B_z and (b) V_x (colar) viewed from the +Z direction. Figure 5.7a shows the position where a change of the IMF direction from positive to negative is the DD. On the other hand, Figure 5.7b reveals the position of the bow shock where the Earthward plasma velocity rapidly decreases (c.f. section 1.1). From these two figures, it is evident that the anti-Earthward current flows along one side along the DD and the other side along the bow shock. The generation mechanism of the perpendicular current on the DD side was clarified in section 5.2.2. At the bow shock, plasma is heated and compressed across the shock wave, and the solar wind kinetic energy is converted to the thermal and electromagnetic energy (Ramon, 2018). This current system exists always present, and its direction frequently varies depending on the Z-direction of the IMF crossing the Bow shock. In Figure 5.7, the southward IMF lines are crossing the Bow shock, so the current at the Bow shock flows towards the dawnside (Hamrin et al., 2018). Therefore, the perpendicular current on the anti-Earthward side of the DD forms the current circuit between the DD and the Bow shock when the DD moves through the dayside magnetosheath region.

On the other hand, we discuss the current circuit on the Earthward side of the DD. Figures 5.7a and b indicate that the current into and out of the DD continues to flow along the bow shock. However, we note that this current does not necessarily flow indefinitely far along the bow shock. This is because these figures only visualized J_{perp}, the perpendicular component of the current, and do not take into account the current parallel (J_{para}) to the magnetic field. Fedder et al., (1997), Siebert and Siscoe, (2002), Siscoe and Siebert (2006), and Guo et al (2008) suggested that the bow shock may contributes to the region 1 Field-Aligned Current (FAC). Therefore, there is a possibility that the J_{perp} converts to the J_{para} in certain localized bow shock regions.

Additionally, this thesis discusses whether both the J_{perp} on the Earthward and anti-Earthward sides of the DD, cross and merge at the DD. If there are a plane with a magnetic field strength of exactly 0 nT, the current generally cannot flow in this plane. Section 5.1 demonstrated that there is a thin YZ plane of the nearly zero magnetic field at the center of the DD. Incidentally, the spread of this plane in the Y-Z direction is much wider than the typical YZ plane of the bow shock. This implies that these J_{perp} cross and merge little at the DD.

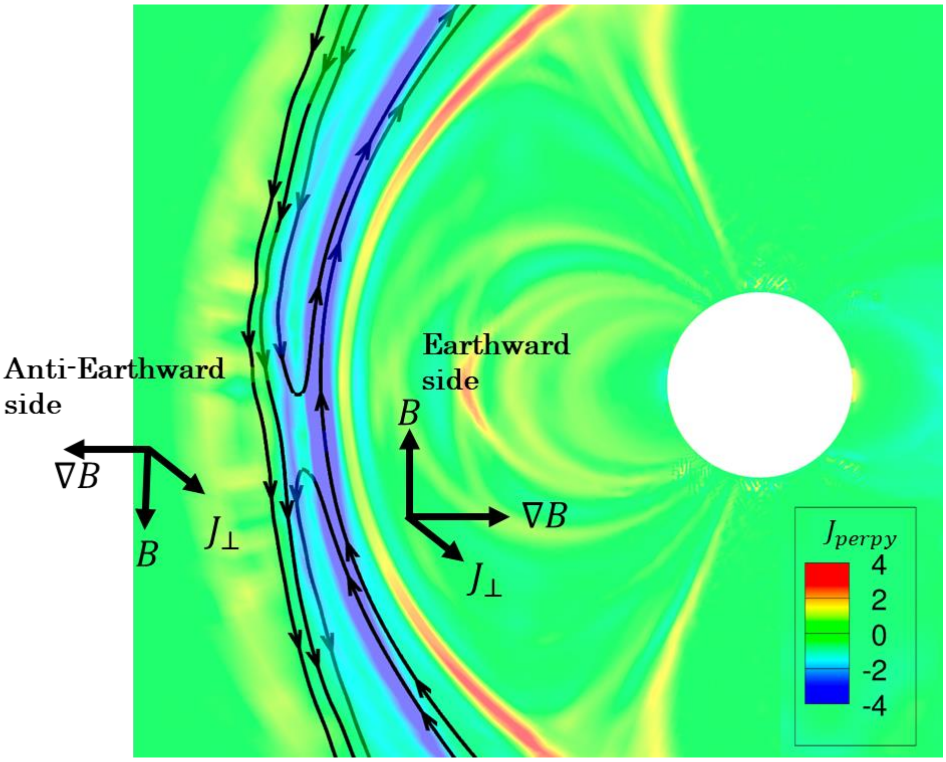

Figure 5.6 The reproduction of the magnetosphere/magnetic field configuration (black lines) and the distribution of the Y-component of the current perpendicular to the magnetic field (contour colors) in the noon-midnight meridian plane (T=4). The X-axis points to Earth, the Y-axis is toward the dusk ward side, and the Z-axis represents the north direction. The central white circle shows the Earth (2.6 Re).

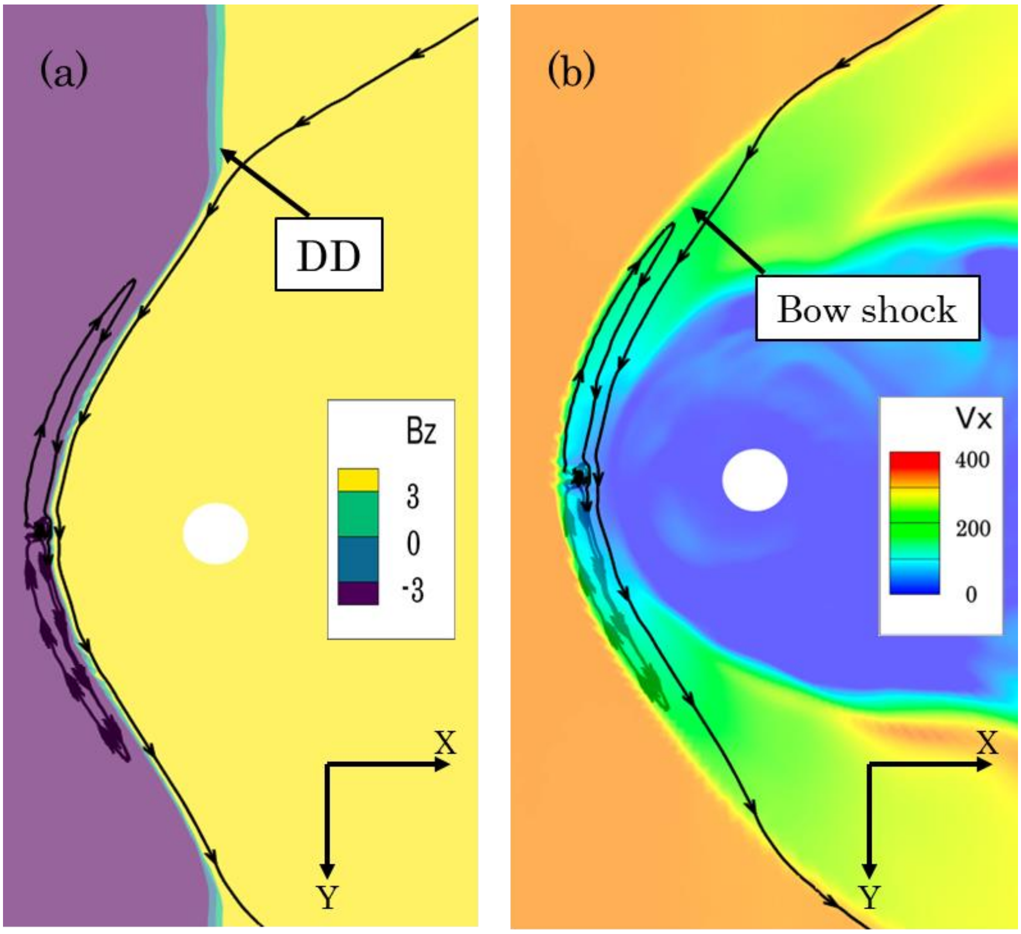

Figure 5.7 The reproduction of the current perpendicular to the magnetic field line (black lines) in the dawn-dusk equatorial plane (T=4). (a) the distribution of the Z-component of the magnetic field and (b) the X-component of the plasma velocity (contour colors). The X-axis points to Earth, the Y-axis is toward the dusk ward side, and the Z-axis represents the north direction. The central white circle shows the Earth (2.6 Re).

6. Time Scale of Disruption of Accumulated Northward IMF Due to Change in IMD Parameter

The northward IMF lines accumulated in the dayside magnetosheath and magnetopause when these lines continued to blow towards the Earth for a long period. Subsequently, new southward IMF lines arrived at bow shock, where they reconnected with accumulated northward IMF lines. This IMF reconnection continuously occurs until the accumulated northward IMF is entirely disrupted. In other words, this IMF reconnection persistently reduces the accumulated northward IMF. Therefore, we examined the timescale until the complete disruption of the northward IMF under a change in southward IMF parameters. Samsonov et al. (2018) reported the effect of the similar timescale when the preceding northward IMF parameter changed. This study utilized both MHD simulations and observations to investigate the time it takes for the southward turning of the IMF to propagate through the magnetosheath. The results showed that an increase in solar wind velocity led to a decrease in the magnetosheath thickness and a reduction in propagation time. Conversely, an increase in IMF strength resulted in an increase in the magnetosheath thickness and a longer propagation time. In this thesis, we simulated various different southward IMF parameters. The southward IMF parameter, the solar wind velocity V_x = 370 km/s, IMF B_z = -3 nT, and the density ρ = 5 cm^{-3}, called run 1. Based on run1, we made five other runs under a change in: the IMF B_z from -3 to -7nT in run 2, the V_x from 370 to 480 km/s in run3, the V_x from 370 to 260 km/s in run4, the ρ from 5 to 7 cm^{-3} in run 5, and the ρ from 5 to 3 cm^{-3} in run 6, respectively. Finally, the timescale was measured from the moment the IMF DD reached the bow shock to the moment all accumulated northward IMF disrupted.

6.1 Results of Change in Southward IMF Parameter

Table 6.1 displays the timescale required for the complete disruption of accumulated northward IMF lines in each run. As these results, the shortest time was 5 minutes in run 3, while the longest was 12 minutes in run 4, indicating a significant time lag of 7 minutes. Additionally, the typical transit time for solar wind plasma through the dayside magnetosheath is about 2-3 minutes. Compared to this timescale, all simulation results showed a certain delay. Huang et al, (2000) reported that the DD propagation time from the bow shock to the magnetopause was estimated by 8 minutes. Taylor et al. (1998) also estimated by 8 minutes when the time requested for passing through the magnetosheaath. These proposed time scales are close to our results.

Run number	Velocity (km/s)	IMF Bz (nT)	Density (cm^{-3})	Time (minute)
1	370	-3	5	8
2	370	-7	5	7.5
3	480	-3	5	5
4	260	-3	5	12
5	370	-3	7	6.5
6	370	-3	3	8.5

Table 6.1 List of the IMF input parameter in this simulation

6.2 Factor to Reduce Accumulated Northward IMF Lines

The propagation time from the bow shock to the dayside magnetopause showed significant variation, as indicated in Table 6.1. Run 2, which involved an increase in the Z-component of the IMF strength compared to run 1, resulted in a slightly shorter propagation time. This reason is believed to be caused by changes in the IMF reconnection outflow. As mentioned in section 4.1, the reconnection outflow typically corresponds to the magnetic field's Alfvén velocity. In run 2, an increase in the magnetic field strength resulted in the faster Alfvén velocity, namely the faster reconnection outflow. Consequently, magnetic field lines after the IMF reconnection (so-called U-shaped magnetic field) can quickly move downstream, and the IMF reconnection frequency increases. This leads to a decrease in the number of accumulated northward IMF lines, shortening the propagation time. However, this effect is not particularly significant in comparison other factors.

Next, run 3 and 4 involved changes in solar wind velocity compared to run 1. Solar wind velocity had the most significant impact factor on propagation time. There are two main reasons for these results. Firstly, changes in solar wind velocity greatly contribute to the background magnetosheath flow velocity. The supersonic solar wind velocity decelerated to the subsonic velocity at the bow shock, but this deceleration never converges to a constant value; the faster/slower the solar wind, the faster/slower background magnetosheath flow. Since the background magnetosheath flow determines the speed at which the IMF DD and the U-shaped magnetic field move towards the Earth, faster magnetosheath velocity results in shorter propagation timescales. The second reason is the change in the solar wind dynamic pressure. If the solar wind velocity increases/decreases, the dynamic pressure also increases/decreases, and compressing/expanding the accumulated northward IMF lines. Compression/expansion effects on the thickness of these lines. Due to these two factors, solar wind velocity is a significant contributor to the propagation time of the DD.

Finally, run 5 and 6 involved changes in solar wind density compared to run 1. Changes in solar wind density primarily contribute only to changes in solar wind dynamic pressure. The influence of the solar wind dynamic pressure on the propagation time has been previously mentioned. In addition, the reason for the smaller variation in propagation time in runs 5 and 6, compared to runs 3 and 4, is due to the absence of changes in the background magnetosheath flow velocity.

Summary and Conclusions

In this study, we reproduced the IMF reconnection phenomenon between the northward and southward IMFs. We revealed that the reconnected magnetic field lines occurred during their motion from dayside to nightside. Through numerical simulations, the northward IMF lines were initially accumulated during 110 minutes in the dayside magnetosheath. Afterward, the accumulated northward IMF region was disrupted due to the incoming southward IMF reaching the bow shock, thereby creating the IMF reconnection. We called the generated magnetic field line after this IMF reconnection the "U-shaped magnetic field line." Then, the IMF reconnection occurred continuously from the bow shock to the dayside magnetopause. Subsequently, the width of the accumulated northward IMF lines gradually decreased. Finally, the Dungey-cycle-reconnection began after the complete disruption of these northward IMF lines by the incoming southward IMF.

We also revealed that the U-shaped magnetic field lines were transported to the high latitude magnetopause and reconnected with the lobe magnetic field lines. This reconnection mechanism connected the U-shaped magnetic field lines to the Earth. We called the magnetic field line after this reconnection between the U-shaped magnetic field and the lobe magnetic field lines the "S-shaped magnetic field line." Moreover, the IMF reconnection's outflow velocity was less than the Dungey-cycle-reconnection and the nightside reconnection outflow velocities. Specifically, a plasma flow velocity increased by 20km/s in the simulation and 75km/s in the Geotail observation relative to the background magnetosheath flow velocity. The reason for this low outflow velocity was the weak upstream magnetic field strength in the IMF reconnection region. Hence, the reconnected magnetic field line (=U-shaped magnetic field line) did not move downstream from the reconnection region effectively. In the end, the IMF reconnection occurred intermittently, confirmed by the plasma flow perpendicular to the magnetic field.

In addition, we elucidated that the current circuit around the DD. In this simulation, we employed the IMF conditions which a change in the direction from northward to southward within one minute. However, there was formed a significantly weaker magnetic field at the center of a YZ plane of the DD. This near zero magnetic field plane effected on the magnetic tension, the magnetic pressure, and the generation of the new current circuit. In particular, the magnetic pressure was most effective generation of the perpendicular current circuit in regions slightly away from the center of the IMF DD toward the Earthward and anti-Earthward sides. Both side's currents formed the circuit between the DD and the bow shock.

Finally, we clarified the time scale of the completely disruption of the accumulated northward IMF associated with a change in the southward IMF parameter. In this simulation, we changed the velocity, density, and magnetic field strength of the southward IMF. As these results, the timescale varied widely between 5 and 12 minutes. These time lags were controlled by three factors: (i) fluctuations in the velocity of the ambient magnetosheath flow, (ii) alterations in the reconnection outflow velocity, and (iii) the compression and expansion of the accumulated region influenced by dynamic pressure.

In regard to future work, it is recommended to consider the impact of the IMF DD on the ionosphere. For instance, by comparing ionospheric potential structures in simulation results with observation data, quantitative understanding of the effects of IMF DD at ground level can be achieved. This result also develops the Sun-Magnetosphere-Ionosphere (S-M-I) coupling system. Furthermore, in this thesis, only a single event of IMF reconnection outflow was observed. These reasons are a little infrequent occurrence of the IMF DD, and the frequent unavailability of satellites in positions where they can observe these effects. However, multiple observation satellites have been launching recently, this limitation is expected to be resolved soon.

Acknowledgement

First of all, I am deeply thankful to my supervisor, Professor Akimasa Yoshikawa. His accurate advice and continuous guidance always supported me in many situations. I learned the attitude of challenging unknown problems and the fun of exploration from him. I would like to express my gratitude to Professor Masakazu Watanabe and Professor Hideki Kawano for their great comments and encouragements. Their useful advice led my research to dramatically develop. I am grateful to Dr. Takashi Tanaka for helpful comments and development of REPPU code used this research. I express my appreciation to Dr. Aoi Nakamizo for the effective discussions and important comment with my thesis. I would like to appreciate to the Dr. Shuji Abe for his technical support about programing. I also thank Dr. Kirolosse Girgis for checking and suggesting the usage of my English. My simulation calculation is used the supercomputer of ACCMS, Kyoto University. We also used the computer resource offered under the category of General Projects by Research Institute for Information Technology, Kyushu University. In addition, our work was supported by JST SPRING, Grand Number JPMJSP2136. I could do my works efficiently by these supports.

Finally, I would like to thank my family for their support and encouragement to my student life.

List of References

・Bhaskar, A., & Vichare, G. (2013). Characteristics of penetration electric fields to the equatorial ionosphere during southward and northward IMF turnings. Journal of Geophysical Research: Space Physics, 118, 4696–4709.

・Birn, J., Borovsky, J. E., Hesse, M., Schindler, K. (2010). Scaling of asymmetric reconnection in compressible plasmas. Physics of Plasma 17, 052108.

・Cassak, P. A., and M. A. Shay (2007), Scaling of asymmetric magnetic reconnection: General theory and collisional simulations, Phys. Plasmas, 14, 102114.

・Dungey, J. W. (1961). Interplanetary magnetic field and the auroral zones. Physical Review Letters, 6(2), 47–48. https://doi.org/10.1103/PhysRevLett.6.47

・Dungey, J. W. (1963). The structure of the exosphere, or adventures in velocity space. Geophysics: The Earth's environment (pp. 503–550).

・Eriksson, E., Vaivads, A., Alm, L., Graham, D. B., Khotyaintsev, Y. V., & André, M. (2020). Electron acceleration in a magnetotail reconnection outflow region using magnetospheric multiscale data. Geophysical Research Letters, 47(1), e2019GL085080.

・Erkaev, N. V. (1988). Results of an investigation of MHD-flow around the magnetosphere. (Review). Geomagnetism and Aeronomy, 28, 529–541.

・Fedder, J. A., S. P. Slinker, J. G. Lyon, C. T. Russell, F. R. Fenrich, and J. G. Luhmann (1997), A first comparison of POLAR magnetic field measurements and magnetohydrodynamic simulation results for field-aligned currents, Geophys. Res. Lett., 24, 2491–2494.

・Fujimoto, M., Nakamura, M. S., Nagai, T., Mukai, T., Yamamoto, T., & Kokubun, S. (1996). New kinetic evidence for the near-Earth reconnection. Geophysical Research Letters, 23(18), 2533–2536.

・Guo, X. C., Wang, C., Hu, Y. Q., & Kan, J. R. (2008). Bow shock contributions to region 1 field-aligned current: A new result from global MHD simulations. Geophysical Research Letters, 35, L03108.

・Hamrin, M., Gunell, H., Lindkvist, J., Lindqvist, P.-A., Ergun, R. E., & Giles, B. L. (2018). Bow shock generator current systems: MMS observations of possible current closure. Journal of Geophysical Research: Space Physics, 123, 242–258.

・Huang, C.-S., Murr, D., Sofko, G. J., Hughes, W. J., & Moretto, T. (2000). Ionospheric convection response to changes of interplanetary magnetic field B_z component during strong B_y component. Journal of Geophysical Research, 105, 5231–5244.

・Imber, S. M., Milan, S. E. & Hubert, B. The auroral and ionospheric flow signatures of dual lobe reconnection. Ann. Geophys. 24, 3115–3129 (2006)

・Koga, D., Gonzalez, W. D., Souza, V., Cardoso, F. R., Wang, C., & Liu, Z. (2019). Dayside magnetopause reconnection: Its dependence on solar wind and magnetosheath conditions. Journal of Geophysical Research: Space Physics, 124(11), 8778–8787.

・Maynard, N. C., Sonnerup, B. U. Ö., Siscoe, G. L., Weimer, D. R., Siebert, K. D., Erickson, G. M., et al. (2002). Predictions of magnetosheath merging between IMF field lines of opposite polarity. Journal of Geophysical Research, 107(A12), 1456.

・Maynard, N. C., Burke, W. J., Ober, D. M., Farrugia, C. J., Kucharek, H., Lester, M., et al. (2007). Interaction of the bow shock with a tangential discontinuity and solar wind density decrease: Observations of predicted fast mode waves and magnetosheath merging. Journal of Geophysical Research, 112, A12219.

・Ogino, T., R. J. Walker, and M. Ashour-Abdalla (1986), An MHD simulation of the effects of the interplanetary magnetic field By component on the interaction of the solar wind with the earth's magnetosphere during southward interplanetary magnetic field, J. Geophys. Res., 91, 10,029.

Phan, T. D., Paschmann, G., Twitty, C., Mozer, F. S., Gosling, J. T., Eastwood, J. P., et al. (2007). Evidence for magnetic reconnection initiated in the magnetosheath. Geophysical Research Letters, 34(14), L14104.

・Ramon, E. Lopez. (2018). The bow shock Current System. In Electric currents in geospacer and beyond.

・Ruohoniemi, J. M., & Greenwald, R. A. (1998). The response of high-latitude convection to a sudden southward IMF turning. Geophysical Research Letters, 25, 2913–2916.

・Russell, C. T. (1972). The configuration of the magnetosphere. Critical problems of magnetospheric physics, edited by E.R. Dyer, 1–16, Inter-Union Comm. on Solar Terr. Phys. Secr., Natl. Acad. of Sci., Washington, D. C.

・Samsonov, A. A., Němeček, Z., Šafr.nkov., Šafránková, J., & Jelínek, K. (2012). Why does the subsolar magnetopause move sunward for radial interplanetary magnetic field?. Journal of Geophysical Research, 117, A05221.

・Samsonov, A. A., Sibeck, D. G., Dmitrieva, N. P., & Semenov, V. S. (2017). What happens before a southward IMF turning reaches the magnetopause? Geophysical Research Letters, 44(18), 9159– 9166.

・Samsonov, A. A., Sibeck, D. G., Dmitrieva, N. P., Semenov, V. S., Slivka, K. Y., Šafránková, J., & Němeček, Z. (2018). Magnetosheath propagation time of solar wind directional discontinuities. Journal of Geophysical Research: Space Physics, 123, 3727– 3741.

・Siebert, K. D., and G. L. Siscoe (2002), Dynamo circuits for magnetopause reconnection, J. Geophys. Res., 107(A7), 1095, doi:10.1029/2001JA000237.

・Siscoe, G. L., and K. D. Siebert (2006), Bimodal nature of solar wind-magnetosphere-ionosphere-thermosphere coupling, J. Atmos. Sol. Terr. Phys., 68, 911–920.

・Spreiter, J. R., & Alksne, A. Y. (1969). Plasma flow around the magnetosphere. Reviews of Geophysics, 7(1–2), 11–50.

・Tanaka, T. (1994), Finite volume TVD scheme on an unstructured grid system for three-dimensional MHD simulation of inhomogeneous systems including strong background potential fields, J. Comput. Phys., 111, 381.

・Tanaka, T. (1999). Configuration of the magnetosphere-ionosphere convection system under northward IMF conditions with nonzero IMF B_y. Journal of Geophysical Research, 104(A7), 14,683–14,690.

・Tanaka, T., Obara, T., & Kunitake, M. (2004). Formation of the theta aurora by a transient convection during northward interplanetary magnetic field. Journal of Geophysical Research: Space Physics, 109, A09201.

・Tanaka, T., A. Nakamizo, A., Yoshikawa, S. Fujita, H. Shinagawa, H. Shimazu, T. Kikuchi, and K. K. Hashimoto (2010), Substorm convection and current system deduced from the global simulation, J. Geophys. Res., 115, A05220, doi:10.1029/2009JA014676.

・Tanaka, T. (2015). Substorm Auroral dynamics reproduced by the advanced global M-I coupling simulation. In Y. Zhang (Ed.), Auroral dynamics and space weather, Geophysical monograph series (Vol. 215, pp. 177–190). AGU.

・Taylor, J. R., Cowley, S. W. H., Yeoman, T. K., Lester, M., Jones, T. B., Greenwald, R. A., et al. (1998). SuperDARN studies of the ionospheric convection response to a northward turning of the interplanetary magnetic field. Annales Geophysicae, 16(5), 549–565.

・Zwan, B. J., & Wolf, R. A. (1976). Depletion of solar wind plasma near a planetary boundary. Journal of Geophysical Research, 81(10), 1636–1648.